Design of ruthenium nanoparticles for better performance in catalysis

Nuria Romero, M. Rosa Axet, Karine Philippot

Design of ruthenium nanoparticles for better performance in catalysis

Nuria ROMERO, M. Rosa AXET* and Karine PHILIPPOT*

CNRS, LCC (Laboratoire de Chimie de Coordination), UPR8241, Université de Toulouse, UPS, INPT, F-31077 Toulouse cedex 4, France

E-mail : nuria.romero@lcc-toulouse.fr ; rosa.axet@lcc-toulouse.fr ; karine.philippot@lcc-toulouse.fr

ORCID numbers

Nuria ROMERO: 0000-0002-2704-7779

M. Rosa AXET: 0000-0002-2483-1533

Karine PHILIPPOT: 0000-0002-8965-825X

Keywords

nanochemistry; ruthenium-based nanoparticles; catalysis; hydrogenation; hydrodeoxygenation; CO_2 reduction; deuteration; hydrogen evolution reaction; oxidation; amine synthesis; reverse and semi-water-gas shift reaction

Abstract

This chapter focus on recent advances in the design of ruthenium-based nanoparticles using organometallic complexes as the metal source, for their application in catalysis. The aim is to illustrate the advantages of the organometallic approach to achieve nanoparticles with controlled characteristics. The adjustment of the morphology (size, shape, crystalline structure) and of the surface

state of metal nanoparticles, are key parameters for the tuning of their catalytic properties. Study and rationalize the effects of these parameters provides interesting perspectives to improve the performance of nanocatalysts. At the laboratory scale, the accurate design of metal nanoparticles is feasible by an adequate choice of the reaction conditions including the nature of the metal precursor (organometallic complex with appropriate kinetics of decomposition), the nature of the stabilizer (polymers, dendrimers, ligands, ionic liquids, etc.), the addition of a second metal for a synergy effect or the use of a support that will bring other properties (stability, conductivity, electronic effects by phosphorus- or nitrogen doping, confinement effect). The challenge is to find the best compromise to achieve robust metal nanoparticles with high catalytic performance, both in terms of activity and selectivity. This will be illustrated through recent examples of ruthenium nanoparticles implemented in catalytic reactions that can find applications in fine chemistry and energy. The complementarity between computational and experimental chemistries, when available, will be underlined, being a powerful way to precisely understand the catalytic properties of nanoparticles and then, improve performance.

Introduction

Interests of metal nanoparticles

As the result of remarkable efforts in the synthesis of precisely defined metal nanoparticles including an atomic precision level,[1, 2] as well as the study of their characteristics, metal nanoparticles (MNPs) have gained a great reputation in the domain of catalysis.[3] MNPs are attractive species because of their unique electronic and structural properties that derive from their matter state (finely divided metals) and a particle size in the nanometric scale (1-100 nm), and confer them typical physical and chemical properties, compared to bulk metals and molecular complexes.[4] MNPs display a high number of surface atoms (high surface to volume ratio; this ratio increasing with size decreasing), among which numerous low-coordination and high-energy atoms.[5] When MNPs are at a size close to one nanometer,

the percentage of surface atoms can be superior to 90%, thus offering a significant number of atomic sites, and making MNPs to be systems of high potential for catalytic transformations.[6] Owing to their different coordination numbers that depends on their location on the NP surface (corner, edge, and face atoms), the atomic sites exposed in MNPs may have various reactivities. Also, according to the MNP shape, different crystalline plans can be exposed at the surface, making the crystalline structure a parameter to consider since different catalytic properties can be achieved as a function of the exposed crystalline plans.[7, 8] However, at very low size (*ca*. 1 nm or below), MNPs can be amorphous and not present well-defined facets but numerous defects, which can be another advantage in catalysis.[9] The composition of MNPs is another key-parameter. If the nature of the metallic core often depends on the target reactivity (some metals are well-known for certain catalytic applications but not for others), the nature of the stabilizer is also of prime importance as, apart from stabilising MNPs, it can influence their catalytic properties. For colloidal catalysis in solution, stabilizers such as polyols, polymers, ligands, macrocyclic host molecules, dendrimers, or ionic liquids (ILs), as non-exhaustive examples, are largely used.[10] For instance, a recent review focused on the use of cucurbit[n]urils (CB[n]s, n = 5–8, 10, 13–15), a family of highly symmetrical, rigid, pumpkin-shaped macrocyclic host molecules, consisting of "n" glycoluril units bridged by methylene groups, generating polar and hydrophobic internal cavity fringed by negatively charged carbonyl groups on two hydrophilic portals to grow MNPs for diverse applications like catalysis.[11] For supported nanocatalysis there is a vast choice of supports (metal oxides such as silica, metal organic frameworks, carbon derivatives, nanocelluloses, etc.) which can be advantageous not only for the recovery and recycling of the nanocatalysts but also for their catalytic properties. For example, MNPs have been immobilized on molecularly modified surfaces, in order to access controlled catalysis.[12] A synergy effect can be expected by combining two metals (or even more), given rise to numerous possibilities of bimetallic NPs for various catalytic applications.[13] Diminution of content or replacement of noble metals by less critical ones, in terms of abundance and cost, is one of the challenges in this domain.

The interest of MNPs in catalysis has been exploited for a long time by the community of heterogeneous catalysis, which mainly focused on naked supported MNPs for a gain in activity. Calcination can be applied to eliminate adsorbed organics and to have free active sites; such a treatment on small MNPs can be critical due to potentially sintering. Selectivity objectives are often treated by a careful choice of the support that brings its own properties (acidic or basic sites, various doping, conductivity, confinement effects, etc.).[14, 15] The target in nanocatalysis is to take advantage of the knowledge in homogeneous catalysts and combine it with that on heterogeneous ones, in order to develop tailored MNPs with high performance in terms of both activity and selectivity.[16] In this perspective, the presence of organic ligands at MNP surface is not seen as detrimental for catalysis but as a way to improve or even orientate the chemoselectivity, as done in molecular catalysis where specific ligands can be used to improve performance of metal complexes.[17, 18] The interaction of ligands with the metal atoms at the surface of MNPs can be seen as similar as that with metal centers in molecular complexes. This interaction is essential for MNP stability and their catalytic performance (activity and selectivity properties). Ligands can be chosen in order to tune the surface properties of MNPs through steric and/or electronic effects.[19, 20] The challenge is to find a suitable protective agent that will stabilize well-defined MNPs while controlling accessibility at the metal surface and catalytic performance. Present developments in nanochemistry rely on the design of nanohybrids (combination of a metal core and a stabilizer or a support, both bringing properties) to have multifunctional nanomaterials.[21]

Given the above, MNPs are structure-sensitive. Their catalytic performances are related to both the characteristics of the metal core (nature, size, shape, morphology) and of the stabilizing shell (organics or support material). Consequently, it is necessary to have efficient synthesis methods to access well-defined MNPs for probing their pertinence in catalysis.

Advantages of the organometallic approach for the synthesis of metal nanoparticles

A prerequisite to finely investigate the catalytic properties of MNPs is to have at disposal synthesis tools that enable to produce MNPs with a well-defined structure (narrow size distribution, appropriate atom distribution in metal core and synergy between the metal surface and stabilizer or support) in a reproducible way. Also, have MNPs of small size (high surface area) will boost the catalytic performance. The organometallic approach (Figure 1) proved to be an efficient and versatile synthesis strategy to access well-controlled MNPs of various metals, with modulable sizes including ultra-small size (ca. 1-10 nm), and that can be functionalized at will.[22, 23] This method relies on the decomposition of organometallic or metal-organic complexes through reduction or ligand displacement from the metal coordination sphere, under mild conditions (most often at ambient or low temperature, and low pressure of hydrogen). Olefinic complexes are suitable precursors because, when exposed to hydrogen, only alkanes are released; these by-products interact poorly with the surface and can be easily eliminated under vacuum. This allows to have a metal surface free of contaminants (absence of halides in contrast to using metal salts, for instance). This is particularly interesting to perform precise studies on the impact of the added stabilizer on the surface properties of MNPs and consequently, on their catalytic performance. If this method suits well to the use of ligands (including polyols,[24, 25] amines,[26] carboxylic acids,[27] phosphines,[28] carbenes,[29] among others) to produce stable MNPs, is because they can easily coordinate at the surface atoms as ligands do in metal complexes. However, various other stabilizers can be used too, such as polymers,[30] ILs,[31] or metal complexes.[32] The stabilization can derive from covalent bonds (organic ligands or metal complexes), electrosteric interaction (surfactants) or electrostatic confinement (certain ILs). MNPs synthesized by the organometallic method can be also deposited onto inorganic supports (carbon-based materials including N- or P-doped materials, metal oxides of various natures such as silica or alumina, etc.), either by direct decomposition of the metal complex chosen as precursor in the presence of the support (and additional stabilizer if required) or by impregnation of the support with a colloidal suspension of preformed MNPs. The organometallic approach also allows the engineering of bimetallic NPs with a control chemical order (alloy or core-shell type NPs) when adequate precursors are available. The deal

is to combine two precursors with appropriate kinetics of decomposition to access the desired bimetallic structure. The versatility of the organometallic approach and all the advantages that provide in order to study metallic surfaces, and in particular in catalysis, have made of this method a success in the scientific community, being adopted by numerous research groups nowadays.

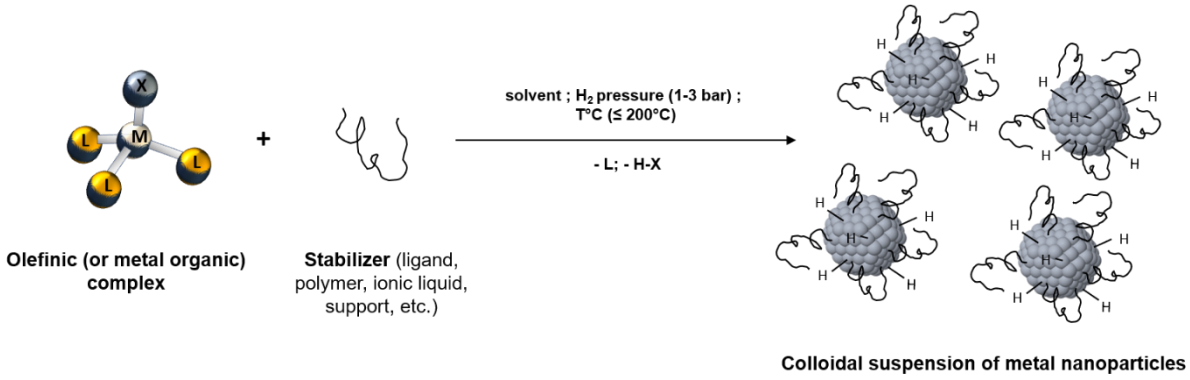

Figure 1. Schematic view of the organometallic approach for the synthesis of metal nanoparticles.

The organometallic approach is particularly performant to access well-controlled ruthenium nanoparticles (Ru NPs), providing a rich literature in this domain.[33, 34] $[Ru(\eta^3\text{-}C_4H_7)_2(\eta^4\text{-}C_8H_{12})]$ and $[Ru(\eta^4\text{-}C_8H_{12})(\eta^6\text{-}C_8H_{10})]$ are relevant precursors to access well-defined and small-sized Ru NPs. Apart from the precursor, it has been reported that the crystalline structure of Ru NPs can be directed by the choice of the stabilizer; in similar synthesis conditions and starting from $[Ru(\eta^4\text{-}C_8H_{12})(\eta^6\text{-}C_8H_{10})]$; hexadecylamine provided Ru NPs with hcp structure while lauric acid gave rise to fcc Ru NPs.[35]

A combination of techniques from both solid and molecular chemistry such as transmission electron microscopy (TEM), high resolution electron microscopy (HREM) or scanning transmission electron microscopy (STEM) coupled with energy dispersive X-ray (EDX), scanning transmission electron microscopy at high angle annular dark field (STEM-HAADF), X-ray diffraction (XRD), wide-angle X-ray scattering (WAXS), liquid and solid state NMR, Fourier transform IR, thermogravimetric analysis (TGA), inductively coupled plasma (ICP), elemental analysis, magnetic measurements, X-Ray photoelectron spectroscopy (XPS), among others, allows to have a fine characterization of these NPs. This provides detailed information of the NP systems and the metallic surfaces, that may be correlated for a better

understanding of their catalytic properties. Hydrogen being used as reducing agent to synthesize Ru NPs, hydrogen atoms are adsorbed at the metal surface in addition of the stabilizer. The surface hydrides content can vary depending on the others species (stabilizer, solvent) present on the surface of Ru NPs but it is generally higher than 1 (1-1.3 H per surface Ru atom). Computational chemistry dedicated to MNPs contributes also to the understanding of the structure as well as surface and catalytic properties of MNPs, in addition to experimental techniques. For instance, computational tools were combined to solution or solid state NMR techniques in order to determine the coordination mode of carboxylic acid ligands at the surface of Ru NPs.[27, 36] A combination of NMR spectroscopy and DFT calculations was also applied to probe the electronic structure−reactivity relationship on ruthenium step-edge sites from ^{13}CO chemical shift analysis, being Ru NPs highly active catalysts for the Fischer−Tropsch and the Haber−Bosch processes.[37] Solid state ^{15}N and ^{13}C CP MAS NMR spectroscopy together with DFT calculations allowed to study the adsorption of $^{15}NH_3$ and the co-adsorption of $^{15}NH_3$ and CO on hydrogen containing Ru NPs stabilized by a phosphine.[38] Regarding the production of hydrogen by the water-splitting process, computational chemistry can afford values of adsorption energy of H atoms at the surface of model NPs and help to probe the interest of MNPs in this process.[39]

The case studies reported below will present pertinent results in the use of catalysts consisting of Ru NPs prepared by the organometallic approach. A main part will concern hydrogenation of diverse substrates, including model compounds for the valorisation of biomass, for application in fine chemistry or the field of fuels. Hydrodeoxygenation is also widely studied with Ru NPs. CO_2 reduction is also explored with Ru-based nanocatalysts. Deuteration of relevant molecules achieved with Ru NPs, has started to be investigated as well. Water splitting for the production of hydrogen is a challenge in energy, for which catalysts based on Ru NPs have known an increasing interest in the last years. The last part of the chapter will report on miscellaneous reactions catalysed by RuNPs, such as oxidation of nitro compounds, synthesis of allyl and alkylamines and the production of formic acid through a semi-water-gas shift reaction for. Finally, some conclusions and perspectives for the future will be given.

Catalytic applications of organometallic Ru nanoparticles

Hydroconversion

Ru NPs, colloidal or supported, are excellent catalysts for hydrogenation reactions as illustrated by the large panel of substrates that can be reduced in their presence.[10, 33] Usually, Ru NPs synthesised by the organometallic approach are used in hydrogenation of C≡C, C=C, and C=O bonds with H_2 under mild reaction conditions. For colloidal Ru NPs synthesised by this method, in which a large variety of stabilizers can be introduced at their surface, the results in a given hydrogenation reaction provide valuable information to assess the contribution of these compounds at the NP surface in the catalytic performance. Likewise, the effect of the introduction of a second metal can be determined straightforwardly using this information. Other compounds can be reduced in the presence of organometallic Ru NPs, such as nitrocompounds, as well as CO_2.

Hydrogenation and hydrodeoxygenation of molecules containing C≡C, C=C and C=O bonds

Ligand- and polymer-stabilized Ru NPs have found applications as catalysts for several hydrogenation reactions. Most of the stabilizing ligands utilized have been taken from organometallic chemistry.[23, 29, 33] Specifically, N-heterocyclic carbenes (NHC) have emerged as powerful ligands to control the properties of MNPs including their catalytic reactivity.[29] Since the first example of carbene-modified AuNPs,[40] and later that of NHC-stabilized organometallic Ru NPs,[41] an extensive effort has been dedicated to the use of NHC as capping ligands for MNPs for applications in catalysis.[29] The origin of this interest lies in that NHC ligands coordinate robustly onto metallic surfaces: adsorption energies of *ca*. -64 Kcal/mol have been calculated for NHC coordinated to Au surfaces, for instance;[42] and, in addition, the electronic or steric properties of MNPs can be adjusted by modifying their N-substituents or imidazolium structure (Figure 2).

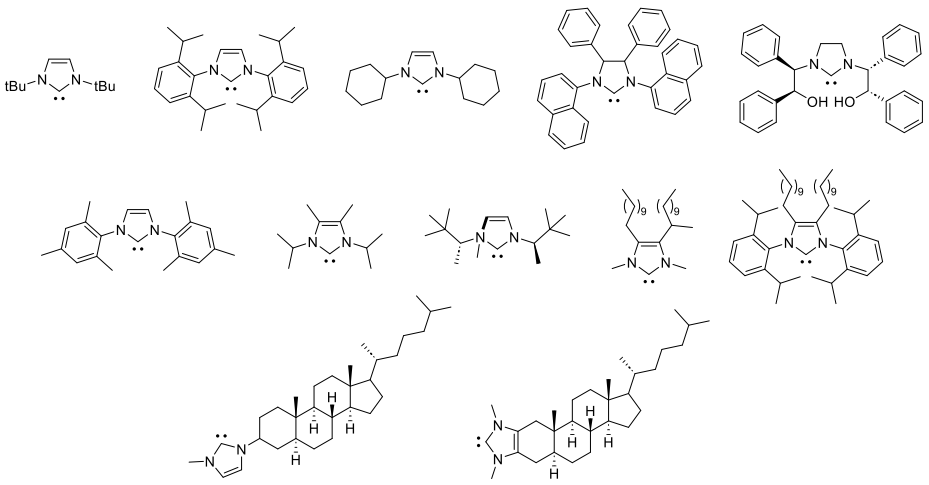

Figure 2. NHC ligands applied as stabilizers of Ru NPs.

1,3-bis(2,6-diisopropylphenyl)imidazol-2-ylidene (IPr) and N,N-di(tert-butyl)imidazol-2-ylidene (ItBu) stabilized Ru NPs were used as catalysts for the hydrogenation of *o*-methylanisole, evidencing that the steric hindrance altered the activity of the reaction, Ru/ItBu being almost inactive.[41] Several attempts to induce enantioselectivity by using chiral NHC stabilized Ru NPs in hydrogenation reactions did not provide the desired result, still the bulkiness of the ligand played an important role to define activity and selectivity.[43, 44] The crucial effect of the steric hindrance of the NHC anchored onto Ru NPs in hydrogenation reactions was evidenced.[45, 46] Long alkyl chain modified NHC, 1,3-dimethyl-4,5-diundecyl imidazoline (LC-IMe) and 1,3-bis(2,6-diisopropylphenyl)-4,5-diundecyl imidazoline (LC-IPr) Ru NPs displayed different activity and selectivity depending on the length of the alkyl chain, being the 2,6-diisopropylphenyl substituted NHC the most active.[46] Cholesterol-derived NHCs were also successfully used as surface modifiers for Ru NPs,[45] providing active catalysts for the hydrogenation of different arenes at mild reaction conditions (room temperature, 5 bar of H_2), the less bulky ligand leading to a better catalytic activity.

Polymer-stabilized MNPs offer the possibility to study the catalytic properties of metallic surfaces without the effect of a ligand, as polymers interact weakly with them. With this particularity, the effect of the addition of a second metal may be investigated unaffected by the presence of a ligand. Besides, the post-synthetic modification of polymer-stabilized MNPs with adsorbates, allows the study of the

effect of ligands on catalysis, preserving the MNPs characteristics defined during the synthesis. Both approaches were recently investigated for applications in upgrading biomass platform molecules.[30, 47] A series of RuNiNPs were synthesised from [Ru(η^4-C_8H_{12})(η^6-C_8H_{10})] and [Ni(η^4-C_8H_{12})$_2$] in the presence of polyvinylpyrrolidone (PVP) at 85°C under H_2 using several Ru/Ni ratios. The RuNi NPs display a segregated structure in which Ni is on the surface, and at low Ni content both metals cohabitate on the surface. The hydrogenation of furfural, performed at 125°C under 20 bar of H_2, was achieved for both RuNi NPs and their corresponding monometallic species. High selectivity towards the partially hydrogenated product, 2-(hydroxymethyl)furan, was observed in all cases, except for Ru/PVP NPs when using 1-propanol as solvent; in this case the heteroaromatic ring could be hydrogenated and opened, and the acetalisation occurred with 1-propanol, thus, reducing the overall selectivity. Synergetic effects between metals were observed on activity, as bimetallic systems were more active than their monometallic counterparts. Additionally, it was observed that the hydrogenation of 2-(hydroxymethyl)furan using Ru/PVP in the presence of 1-propanol, gave 1,2-pentanediol in an interesting 27% selectivity. With the aim to produce 1,2-pentanediol directly from furfural in a competitive amount using Ru/PVP as catalyst, the acetalisation reaction should be reduced drastically. Thus, electron donor ligands were added *in situ* to the catalytic reaction, in order to diminish this side reaction, the origin of which is probably due to the electron-deficient character of the Ru NP surface.[47] As a general trend, the addition of an amine increased the TOF of the reaction, and in the case of hexadecylamine (HDA) it allowed the hydrogenation of furfural towards tetrahydrofurfuryl alcohol, producing as well 1,2-pentanediol by C-O cleavage in a 36% selectivity, avoiding the formation of the acetal, as hypothesised. Other amines, an NHC, and a phosphine ligand did not provide the C-O cleavage, which was tentatively attributed to the bulkiness of the ligands. Upgrading furfural or hydroxymethylfurfural by hydrodeoxygenation was also achieved with MNPs using magnetic heating.[48] The magnetic heating -release of heat through hysteresis losses when ferromagnetic materials are subjected to a high-frequency alternating magnetic field-, was possible using $Fe_{2.2}C$ NPs,[49] as the support of the Ru NPs. The catalyst was prepared through a two-step decomposition of [$Ru_3(CO)_{12}$]

under 1 bar H_2 in the presence of pre-synthesised $Fe_{2.2}C$ NPs. Using 3 bar of H_2, and a magnetic field of 58 mT, 300 kHz for 15 h of reaction, furfural and hydroxymethylfurfural were fully hydrodeoxygenated towards 2-methylfurane and 2,5-dimethylfurane, respectively.

Ru NPs resulting from the decomposition of $[Ru(\eta^4\text{-}C_8H_{12})(\eta^6\text{-}C_8H_{10})]$ under H_2 display, usually, a small size -1 to 2 nm size- and a rather homogeneous size distribution. This was exploited in order to arrange high quality Ru NPs in networks mediated by di- or multitopic ligands, finding applications in catalysis.[50, 51] The strategy of using ligands as directing linkers has been used for obtaining ordered NPs -mostly Au- for several applications such as in optics, sensors and electronics,[52, 53] but barely in catalysis.[54, 55] Yet, such self-assembly of MNPs could permit in a straightforward manner to direct substrates, or to create confined spaces, in addition to the expected effect of the ligand modulating the electronic/steric properties of the MNP surface. In an attempt to create such networks, fullerene C_{60} was used as the directing ligand in the synthesis of Ru[50, 51, 56] and Rh[57] NPs. Even if the nanostructures obtained by hydrogen decomposition of $[Ru(\eta^4\text{-}C_8H_{12})(\eta^6\text{-}C_8H_{10})]$ or $[Rh(\eta^3\text{-}C_3H_5)_3]$ in the presence of fullerene C_{60} did not show the desired organization, the presence of the fullerene C_{60} provided an electro deficient character to the metallic surfaces, which had an impact in catalysis. In order to create directionality carboxylic acid moieties were introduced into the fullerene C_{60},[58] the choice for -COOH groups arising from their robust coordination onto Ru surfaces.[27, 36, 59] Using this multitopic ligand, $C_{66}(COOH)_{12}$, the expected networks were obtained. The Ru NPs tridimensional networks were active for the reduction of nitrobenzene, demonstrating that the metallic surface was available for catalytic transformations. Thus, the methodology was extended to more straightforward ligand structures. Carboxylic acid triphenylene derivatives, planar ligands, provided bidimensional assemblies,[60] as confirmed by electron tomography (ET) and atomic force microscopy (AFM). AFM permitted to identify nanoobjects with a high aspect ratio, the lateral size of the objects ranged from 0.1 to 1 µm, while the thickness arrayed from 3 to 12 nm - the estimated thickness of the assembly corresponding to one to four layers of MNPs. The interparticle distance, ascertained by ET, displayed a mean value of 2.4 ± 1.2 nm, in reasonable agreement with the one determined by SAXS analysis (2.9 nm). Nevertheless, when applied

as catalysts for the acetylene semi hydrogenation, the two-dimensional Ru NPs networks were less performant than tri-dimensional Ru NPs arrays based on fullerene[60] or adamantane[26] ligands. The latter tridimensional Ru NPs networks were straightforwardly assembled using several adamantane-based compounds bearing carboxylic acid or amine functional groups. The Ru interparticle distance was modulated by the bulkiness of the ligand as the RuNP size was roughly the same in all materials, and the functional groups conferred different electronic properties to the RuNP surface, as well as different robustness to the arrays. The adsorption energy of the carboxylate form of 1-adamantane carboxylic acid was calculated to be very robust, -60 kcal/mol, and a charge transfer of -0.84 e^-, from the Ru_{13} NP towards the ligand, was determined, pointing to an electro deficient metallic surface. On the opposite, the adsorption energy of 1-adamantylamine onto a Ru_{13} cluster was found lower, -30 Kcal/mol, and a charge transfer from the donor ligand to the Ru surface of -0.12 e^- was calculated, thus pointing to an electron rich surface. The electronic effects of the different coordinated ligands altered the activity and the selectivity in the semi hydrogenation of phenylacetylene. A relationship between Ru interparticle distance with the catalyst activity was found. Short distances between Ru NPs were correlated to a higher catalytic activity, which was attributed to confinement effects.

ILs are attractive compounds for the synthesis of MNPs as they both stabilize and confer specific features to metallic surfaces and can act as solvent. The modularity of ILs originates from changing functional groups, alkyl chain length, hydrophobicity, varying the ion pair, and so on, and in turn the modulation of the catalytic properties of MNPs.[61, 62] Following a pioneering work on the use of Ir NPs stabilized by ILs as catalysts for hydrogenation reactions,[63] a plethora of stable MNPs, with small size and narrow size distributions, has been synthesised in ILs.[64] Specifically, the reduction of Ru compounds or the decomposition of organometallic compounds dissolved in the imidazolium ILs has been used as a straightforward methodology to produce Ru-based catalysts active in the hydrogenation of several substrates.[65-70] For instance, several alkenes were successfully hydrogenated by using Ru NPs stabilized on 1,3-dialkylimidazolium ILs (Figure 3, left, for some examples), prepared by the decomposition of [Ru(η^4-C_8H_{12})(η^6-C_8H_{10})] under H_2.[65] The difference of solubility of benzene

and cyclohexene in 1-*n*-butyl-3-methylimidazolium hexafluorophosphate (BMIm·PF_6) was exploited in order to attain a high selectivity in the partial hydrogenation of benzene; at very low benzene conversion, a selectivity of *ca*. 39 % in cyclohexene was observed. Ru-based catalysts were also prepared by employing [Ru(η^3-C_4H_7)$_2$(η^4-C_8H_{12})] and 1-n-butyl-3-methylimidazolium or 1-n-decyl-3-methylimidazolium, using N-bis(trifluoromethanesulfonyl)imidates (NTf_2) or tetrafluoroborates (BF_4) as ion pair.[67] The variation of the structure of the IL, the imidazolium cations or the anions, did not have an impact in the outcome of the reaction, and the partial hydrogenation of benzene derivatives towards the corresponding cyclohexene was only observed in trace amounts. Lastly,[70] Ru NPs were successfully produced using [Ru(η^4-C_8H_{12})(η^6-C_8H_{10})] and functionalised imidazolium-based ILs (FILs) and tested in the hydrogenation of styrene. The ILs consisted in a series of 1-substituted 3-methylimidazolium cations and NTf_2 as the ion pair (Figure 3, right). Interestingly, all the Ru/FILs were highly selective to the partial hydrogenated product, ethylbenzene, even at prolonged reaction times. The fact that the aryl moiety is not hydrogenated is unusual for Ru NPs based catalysts that are reported as highly active for this type of reactivity. In addition, the functional group at the end of the alkyl chain had an impact on activity and stability, diether substituted FILs displaying a convenient compromise between both parameters.

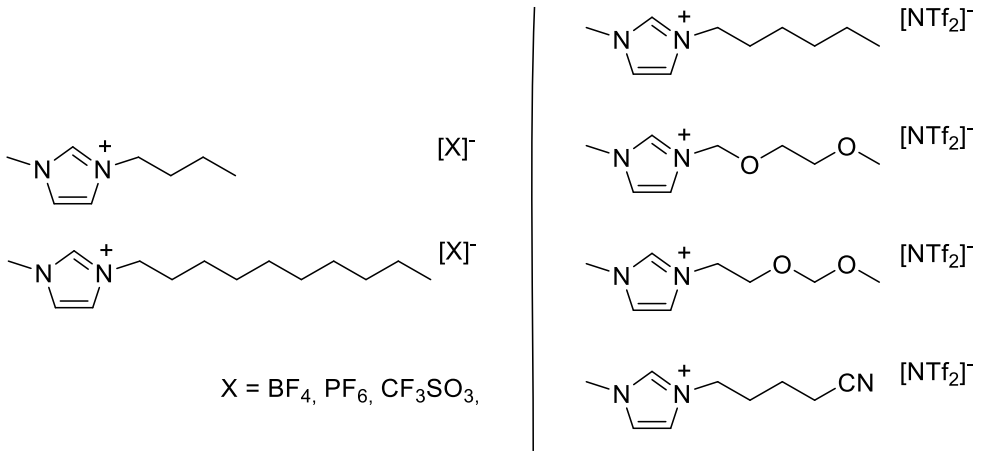

Figure 3. Ionic liquids based on 3-methylimidazolium cations used to synthesize Ru NPs.

The introduction of complexity to the MNPs/ILs nanocatalysts, as in heterogeneous catalysis in general, permits to produce more performant catalytic systems. The addition of a second metal seeking for synergy, or the introduction of supported ionic liquids phase (SILP) nanomaterials pursuing stability and another possibility of tunability *via* the support, have been also explored. For instance, for the former case, core shell RuPt NPs[69] or alloyed RuPd NPs[68] synthesised straightforwardly in ILs by using the organometallic approach showed a synergy between metals in catalytic hydrogenation. RuPt NPs[69] in BMI·PF_6 produced 1,3-cyclohexadiene from benzene, in a 21 % selectivity at 5 % benzene conversion, a reactivity that was not observed for the corresponding monometallic nanocatalysts under the same reaction conditions. A synergy in terms of catalytic activity was observed in the hydrogenation of benzene on alloyed RuPd/ILs NPs.[68] RuPd ratio 1:1 NPs in BMI·PF_6 displayed high activity and selectivity for the hydrogenation of benzene, with 94% and >99%, respectively, at 60°C under 4 bar of H_2, a catalytic performance in contrast with that of RuPd ratio 9:1 and RuPd ratio 1:9, that provided only 68% and 2% of conversion, respectively, under same reaction conditions. The decomposition of ruthenium complexes in SILP materials provides a facile procedure to prepare Ru-based heterogeneous catalysts. SILP materials combine the advantages of ILs (non-volatility, high solvent capacity, etc.), those of heterogeneous support materials, and the possibility to adjust the catalytic properties, or by introducing a second metal, or changing the nature of the ionic liquid, or the support. The nature of the IL plays an important role in the catalytic properties of those materials.[12] For example, [$Ru(\eta^3\text{-}C_4H_7)_2(\eta^4\text{-}C_8H_{12})$] was impregnated in a combination of covalently attached acid-functionalized IL and non-functionalized IL in SiO_2, and decomposed under H_2, the procedure providing small Ru NPs -less than 2 nm.[71] The quantity of sulfonic acid moieties grafted onto SiO_2 was varied in order to achieve several acidities and to assess the impact of this parameter in the Ru-catalysed deoxygenation of several biomass substrates. Higher acid loaded catalysts presented higher catalytic activities for the hydrogenolytic deoxygenation of 4-(2-tetrahydrofuryl)-2-butanol and of 4-(5-(hydroxymethyl)-2-tetrahydrofuryl)-2-butanol, providing quantitative yields of C_8-OL products (1-octanol, 1,1-dioctylether and ethyloctylether). Hydrodeoxygenation of phenolic substrates was

investigated using the same catalytic materials,[72] demonstrating again that the acidity conferred by the IL to the catalysts has an strong impact on the reaction results, as previously reported.[73] Ru NPs@SILPs were investigated for the hydrodeoxygenation of phenol under batch conditions at 150 °C using 120 bar of H_2. The acid loading of the SILP was varied between 0.33 and 1.00; increasing the acidity led to an increase of the activity and a shift in the product selectivity from the alcohol toward the deoxygenated product, cyclohexane. Increasing the temperature to 175°C permitted to obtain 95 % of cyclohexane using Ru NPs@SILP-1.00. The hydrogenolysis of diaryl ethers was also attained with Ru@SILP-SO_3H bifunctional catalyst. The effectiveness of the catalyst depended on the substrate: cycloalkanes were obtained in high yields from diphenyl ether and 4,4'-dimethyldiphenyl ether, but for other more hindered substrates was less efficient. Regioselectivity of the process was also demonstrated for several unsymmetrical compounds in the same reaction conditions.[74] The modification of the SILP was also achieved by introducing a Lewis acid; Ru@SILP-$[ZnCl_4]^{2-}$ was used as catalyst for the hydrogenation of bicyclic heteroaromatic compounds. [75] A comparison with the non-modified SILP showed the beneficial effect of this modification: the presence of the Lewis acid hindered the hydrogenation of arenes, thus promoting selectively towards the hydrogenation of the heteroaromatic ring, and accelerating the hydrogenation of the furan moiety.

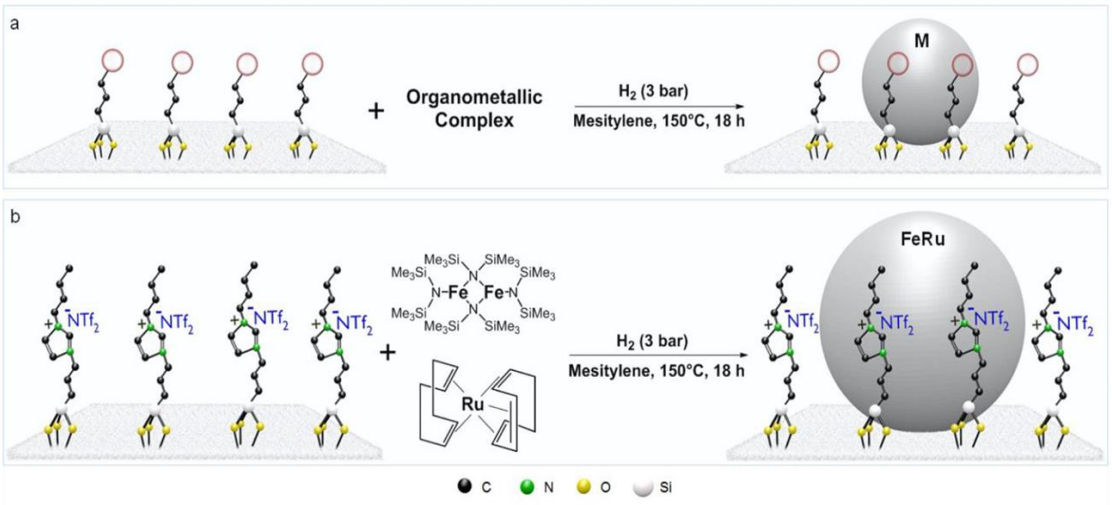

Figure 4. Organometallic synthesis of MNPs on molecularly modified surfaces: (a) general approach; (b) example of bimetallic RuFeNPs immobilized on an imidazolium-based SILP.[76] Adapted from [12].

Supported bifunctional catalysts consisting in Ru NPs immobilized on tertiary amine-functionalized polymer-grafted silica (PGS) were also studied.[77] The use of PGS as a CO_2-responsive material allowed to switch the selectivity of the hydrogenation of furfural acetone by feeding or not the reactor with CO_2. Ru@PGS under pure hydrogen produced mainly 4-(tetrahydro-2-furyl)butan-2-ol, *i. e*. the fully hydrogenated product, from furfural acetone; a mixture of H_2/CO_2 (40 bar, 1:1) led to the exclusive hydrogenation of the C=C bonds, producing 4-(2-tetrahydrofuryl)-butan-2-one. The selectivity switch was induced by the reversible hydrogenation of CO_2. Ammonium formate and ammonium bicarbonate species were detected by means of NMR, demonstrating that the Ru@PGS catalyst is active in the hydrogenation of CO_2 to formic acid -which reacts in turn with the amine-decorated support. The presence of these species was suggested to play a role in the selectivity shift observed after the introduction of CO_2 into the gas feed, by blocking of active sites for the hydrogenation of the more polar C=O group rather than the C=C hydrogenation sites. The preparation of bimetallic NPs is an effective strategy to tune the catalytic properties of heterogeneous catalysts, as the introduction of a second metal induces electronic and strain effects, which alter the catalytic properties when compared to those of the monometallic counterparts. Even if ruthenium is a competitive metal in terms of price compared to other noble metals such as platinum, palladium, and rhodium, there is significant interest in its replacement with third-row metals as an abundant, inexpensive, and environmentally benign alternative to the noble metal catalysts. With this aim, RuFe and RuCo NPs were prepared on covalently attached IL in SiO_2. RuFeNPs@SILP[76, 78-80] and RuCoNPs@SILP[78] catalytic systems were obtained by *in situ* reduction in the presence of unmodified SILP of $[Ru(\eta^4\text{-}C_8H_{12})(\eta^6\text{-}C_8H_{10})]$ and $[Fe[N(Si(CH_3)_3)_2]_2]_2$ or $[Co(\eta^3\text{-}C_8H_{13})(\eta^4\text{-}C_8H_{12})]$, under 3 bar of H_2 at 150°C in mesitylene as a solvent. The metallic ratio on the bimetallic NPs was straightforwardly tailored by controlling the initial amount of the metallic precursors. The hydrogenation of several aromatic compounds including benzylideneacetone, using RuFeNPs@SILP series or the corresponding monometallic species, showed that the presence of Fe fine-tuned the selectivity of the reaction. While FeNPs@SILP were barely active for the hydrogenation under 20 bar of H_2 at 120 °C after 18 h of reaction, Ru NPs@SILP gave the fully hydrogenated product.

The bimetallic material $Ru_{75}Fe_{25}$NPs@SILP hydrogenated several unsaturated functions but not the aromatic rings. By calculating the reaction rates for the hydrogenation of furfuralacetone, using $Ru_{75}Fe_{25}$NPs@SILP or Ru NPs@SILP, it was evidenced that the introduction of Fe impeded hydrogenation of the heteroarene and, at same time, the ketone hydrogenation was enhanced. $Ru_{75}Fe_{25}$NPs@SILP, in which SILP was acid-functionalized[79] or non-functionalized,[80] was also used as hydrodeoxygenation catalyst for several aromatic substrates. Taking advantage of the inability of these catalysts to hydrogenate aromatic rings, aromatic ketones were selectively hydrodeoxygenated at 175 °C under 50 bar of H_2, to the corresponding aromatic deoxygenation products. The catalytic hydrodeoxygenation of hydroxy-, amino-, and nitro-acetophenone derivatives was successfully achieved with $Ru_{75}Fe_{25}$NPs@SILP, using the unmodified covalently bonded IL to silica, to produce selectively alkyl phenols and anilines.[81] The catalyst was also submitted the continuous flow hydrodeoxygenation of 4-hydroxyacetophenone for over 6 h time-on-stream, demonstrating the stability of this catalytic system. Similarly, the introduction of Co to the Ru NPs@SILP structure leading to RuCoNPs@SILP catalyst changed the catalytic properties of pure Ru catalyst.[78] RuCoNPs@SILP was able to hydrogenate selectively benzylideneacetone to produce the aromatic hydrogenated product, while pure Ru-based nanomaterial produced the fully hydrogenated product.

The reduction/decomposition of Ru complexes is a versatile procedure to anchor NPs onto supports, these nanomaterials finding applications as catalysts for hydrogenation reactions. Ru NPs synthesised from $[Ru(\eta^4\text{-}C_8H_{12})(\eta^6\text{-}C_8H_{10})]$ in the presence of nanographenes allowed to characterise the interaction of the Ru NPs with these saddle-shaped molecules, a curved mimic of graphene sheets.[82] It was observed that nanographene interacts via π-π interaction, and DFT calculations pointed to a metal-to-ligand charge transfer, thus providing electron deficient metallic surfaces. Numerous aromatic substrates were successfully hydrogenated with this type of catalyst at mild reaction conditions (10 bar H_2, 50°C). $[Ru(\eta^4\text{-}C_8H_{12})(\eta^6\text{-}C_8H_{10})]$ also generated small Ru NPs upon hydrogenation onto a reduced-graphene oxide (rGO) followed by *in situ* modification of the Ru NPs with an NHC ligand containing a pyrene-moiety (Figure 5).[83] Hydrogenation of acetophenone was investigated using the

so-obtained catalyst, displaying the beneficial effect of the modification with the NHC ligand, in terms of activity and selectivity. Other substrates were also successfully hydrogenated using the NHC modified catalytic system. Ru NPs were also anchored onto reduced-graphene oxide doped with N (NH_2-rGO) or reduced-graphene oxide (rGO) by using the same procedure, *i. e*. direct decomposition of [Ru(η^4-C_8H_{12})(η^6-C_8H_{10})] in the presence of the support.[84] Due to their robustness, these catalysts were applied in the hydrogenation of palmitic acid to 1-hexadecanol at 210°C under 100 bar H_2. The support and specifically the presence of N on it, had an impact on the Ru NPs structure and activity. Ru/rGO NPs were larger and displayed lower catalytic activity than Ru/NH_2-rGO. The hypothesis is that the presence of amino and pyrrolic nitrogen atoms on the support not only conferred stability to the catalyst, but also the basic sites played a role during catalysis by splitting heterolytically the H_2. RuPt NPs were also supported on NH_2-rGO, by decomposing a mixture of [Ru(η^4-C_8H_{12})(η^6-C_8H_{10})] and [Pt(η^2-C_7H_{10})$_3$] under 3 bar of H_2 in the presence of NH_2-rGO.[85] Varying the Ru to Pt ratio was possible to straightforwardly produce a series of alloyed RuPt catalysts, as well as the corresponding monometallic counterparts. Synergetic effects between metals were not observed in the hydrogenation of acetophenone, as monometallic Ru/NH_2-rGO were the more active, but the bimetallic systems displayed an interesting compromise between activity and selectivity. Pre-synthesised MNPs can also be anchored onto a support in a subsequent step. This allows to compare the support effect onto the catalytic performance of the nanomaterials, as the post-addition of the support does not affect the initial properties of the NPs determined during their synthesis, thus, key properties -size, shape, cystallinity, etc- are unaffected. Thus, Ru/PVP, Rh/PVP, and Pd/PVP were synthesised using the organometallic approach and immobilized onto silica-coated magnetite, that was then modified with ceria or titania, by a simple impregnation process.[86] Ru based catalysts were selective towards cyclohexanol in the phenol hydrogenation performed at 75°C under 6 bar of H_2. Slight support effects were observed, the titania-modified catalyst displaying the highest activity.

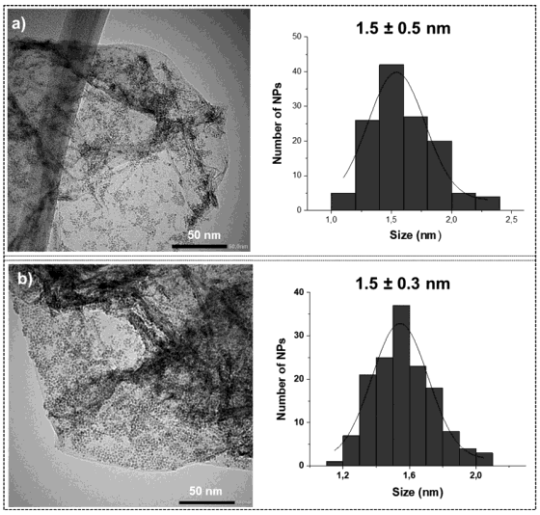

Figure 5. TEM images and size distribution histograms of (a) Ru/rGO and (b) NHC modified Ru-rGO. Adapted from [83].

Reduction of nitro molecules

Ru nanocatalysts prepared from [Ru(η^4-C_8H_{12})(η^6-C_8H_{10})] in the presence of C_{60} under H_2 using several Ru/C_{60} ratios, displayed electron poor Ru surfaces, as pointed out by Raman, XPS, EXAFS and CO adsorption experiments.[50, 51] This feature had an effect on the chemoselective hydrogenation of nitrobenzene.[87] Ru NPs supported on Ru-fulleride nanospheres hydrogenated successively and chemoselectively nitrobenzene to aniline and then to cyclohexylamine. The reaction was studied at 30 bar of H_2 at 80°C in alcoholic solvents and was sensitive to the solvent used, proceeding faster in methanol than in other alcohols. The reduction proceeded selectively on several substituted nitroarenes, proving the scope of the nanocatalyst. DFT calculations confirmed that fullerene confers to Ru an electro deficient character by charge transfer; also pointing to that the high selectivity of the hydrogenation reaction is mainly governed by the presence of surface hydrides on the electron-deficient Ru NPs. A ligand effect was also demonstrated in a subsequent work;[88] fullerene C_{60} provides unique electronic properties to the Ru nanocatalyst containing it, that enhances the catalytic properties, providing a very efficient nitrobenzene reduction. Reactivity towards the hydrogenation of nitrobenzene was used to assess the nature of the Ru species embedded on fullerene C_{60}.[89] By varying the Ru/C_{60} ratio and the reaction solvent during the Ru-C_{60} synthesis, several Ru based nanostructures

may be obtained including single atom, cluster, and NPs based materials. Nevertheless, at small sizes it is difficult to distinguish between small clusters and atomic dispersed atoms. Catalysis results compiled using several Ru-C_{60} nanostructures in the hydrogenation of nitrobenzene and 2,3-dimethyl-2-butene in combination with the data from the characterization techniques and DFT calculations, allowed to fully understand the nature of Ru-C_{60}, pointing that atomically dispersed Ru atoms were possibly present at high Ru loading.

Electrochemical reduction of nitrobenzene was investigated with supported Ru NPs generated from the direct hydrogenation of [Ru(η^4-C_8H_{12})(η^6-C_8H_{10})] in the presence of carbon nanofibers.[90] After 15h of electrolysis at −1 V *vs.* Ag/AgCl reduction of nitrobenzene towards azoxynitrobenzene was achieved with 82.7% selectivity

Hydrogenation of carbon dioxide

CO_2 can be chemically reduced in the presence of H_2 and a catalyst. The CO_2 reduction may be a key solution to both the reduction of the greenhouse effect, and the production of versatile C1 products and hydrocarbons, which are of high interest as energy carriers, and feedstocks for the chemical industry.[91] Ru-based materials are able to dissociate CO, and can act as methanation or Fischer-Tropsch (FT) catalysts, if CO is produced from CO_2 by reverse water-gas shift (RWGS), this tandem reaction can produce methane or hydrocarbons directly from CO_2. Even if Ru-based catalysts are very active for CO reduction, the selectivity is low compared to that of other earth abundant metal-based catalysts. Co- and Fe-based catalysts are selective for the Fischer-Tropsch reaction, while Ni is selective to produce methane, and they are preferred for industrial implementation. In addition to that, Ru catalysts promote the formation of acid formic/formate from CO_2, thus adding more complexity towards a selective catalysis. Nevertheless, heterogeneous Ru-based catalysts have been studied for the reduction of CO2,[33] even if homogeneous systems are still more performant.[92] Works concerning Ru based catalysts are relatively scarce, and most of them deal with the control of selectivity for this process.[33] ILs have emerged as interesting stabilizing agents for Ru NPs as they can tune catalytic

properties and provide thermal stability to the MNPs. In addition, the introduction of functional groups in the ILs, different anions, and so on, can improve solubility of reactants and impact the catalytic performance. Ru-based catalysts stabilized in various ILs have been investigated in CO_2 reduction, exploring the effect of the nature of the IL and the addition of a second metal.[93-95] Firstly, $[Ru_3(CO)_{12}]$ was combined with several ILs bearing basic anions;[93] producing selectively HCOOH from CO_2 at 60°C and 40 bar of pressure (H_2/CO_2 1:1). The ILs stabilized the catalyst, facilitated the formation of bicarbonate when using water, and buffered the reaction media. It has been possible to immobilize the IL of interest on a resin, in order to isolate HCOOH easily from the reaction media. Taking into consideration these results, complexity was added to the catalytic system by synthesizing bimetallic NPs.[94, 95] In this study also, the IL had an important role tuning the selectivity, yet the introduction of the second metal was key to produce methane or higher hydrocarbons. RuFe NPs were prepared co-reducing $[Fe(CO)_5]$ and $[Ru(\eta^3\text{-}C_4H_7)_2(\eta^4\text{-}C_8H_{12})]$ in the presence of 1-butyl-3-methyl-1H-imidazol-3-ium acetate (BMi.OAc), hydrophilic IL, or 1-butyl-3-methyl-1H-imidazol-3-ium bis((trifluoromethyl)sulfonyl)amide, ($BMi.NTf_2$), hydrophobic IL, under 3 bar of H_2 at 150°C.[94] While using the hydrophobic IL, $BMi.NTf_2$, RuFe catalyst displays reactivity from both metals, Ru increases the activity, and Fe increases the selectivity towards higher hydrocarbons through combination of RWGS and FT. A different scenario was observed when performing the CO_2 reduction in $DMSO/D_2O$ solution containing a hydrophilic IL based bimetallic system, RuFe-BMi.OAc, which produced exclusively formic acid, in line with previous work.[93] Monometallic Fe-BMi.OAc did not show any activity in the studied reaction conditions, while monometallic Ru-BMi.OAc produced HCOOH in a molar ratio of 1.18 HCOOH/IL. The addition of Fe into Ru had a positive effect of the activity (1.66 HCOOH/IL) displaying still exclusive formation of formic acid. The tuning of selectivity on CO_2 reduction mediated by hydrophobic IL towards the synthesis of hydrocarbons *via* RWGS + FT, was further investigated using bimetallic RuNi NPs.[95] $[Ru(\eta^3\text{-}C_4H_7)_2(\eta^4\text{-}C_8H_{12})]$, $[Ni(\eta^4\text{-}C_8H_{12})_2]$ and a mixture of both complexes using several Ru/Ni ratios were decomposed in $BMi.NTf_2$ to obtain the desired catalysts. Hydrogenation of CO_2 was conducted at 150 °C under 8.5 bar of pressure (H_2/CO_2 4:1). The

incorporation of the earth abundant metal onto Ru -Ni-BMi.NTf_2 was not active under this catalytic reaction conditions; had a positive effect on the activity, as bimetallic systems displayed higher conversions than the one obtained for Ru-BMi.NTf_2, and modulated the selectivity towards CO and higher hydrocarbons. Interestingly, the use of BMI.BF_4, a hydrophilic IL, promoted the CO production, thus enhanced RWGS. Ru/SILP catalysts were also explored in the reduction of CO_2.[96]. A series of catalysts were synthesised from [Ru(η^3-C_4H_7)$_2$(η^4-C_8H_{12})] in which the SILP phase was varied in the anion or in the functionalisation of the side chains. The anions, Br, OAc, OTf and NTf_2, had hydrophilic, hydrophobic, nucleophilic, and non-nucleophilic properties, and the side chains were neutral, basic, and acidic (-CH_2CH_3, -NH_2, -NEt_2, -$(CH_2)_2SO_3H$). The catalytic reduction was performed at 100°C under 60 bar of pressure (H_2/CO_2 2:1) using a mixture of NEt_3 and water as a solvent. All catalysts were more active than Ru@SiO_2, which proved the beneficial effect of the introduction of the IL. CO_2 conversions ranged from 5 to 18%, and TOFs from 33 to 280 h^{-1}. Ru@SILP(SO_3H-OAc) and Ru@SILP(SO_3H-NTf_2) produced the highest TONs of the series, 1182 and 846, respectively. Further optimisation of the reaction conditions allowed to observe TONs as high as 16100 using Ru@SILP(SO_3H-OAc). The It was pointed out that the presence of ammonium sulfonate species on the SILP had an important role to regulate equilibria between the species at the surface and in solution, which enhanced the catalytic properties.

Photothermal CO_2 methanation was achieved at 250°C using a combination of Ru NPs, which are active and selective for CO_2 methanation, with Au NPs, which exhibit a plasmonic band and can transfer the energy absorbed towards Ru NPs.[97] Au NPs, synthesised from $HAuCl_4$ and oleylamine, were immobilized in Siralox. In a second step, Ru NPs were synthesised on the supported Au NPs, by decomposition of [Ru(η^4-C_8H_{12})(η^6-C_8H_{10})] by H_2. This catalytic system produced exclusively CH_4, as no other products were detected. This catalytic performance results from a synergetic effect between metals; monometallic Au catalyst was inactive for the methanation of CO_2, while monometallic Ru was thermal and photocatalytic active towards this reaction, demonstrating that Ru is responsible for the

catalytic activity. The introduction of Au to the Ru catalyst harvested the visible light absorption and increased the production of CH_4.

As a conclusion, catalysts based on Ru NPs display high performances in hydrogenation and dehydrogenation reactions. Over time, the knowledge acquired from experimental results and theoretical calculations allows nowadays to have in hands high performing nanocatalysts. The understanding of the coordination of ligands and substrates, the addition of a second metal, or the use of ILs or SILPs permit to provide specific and more performant catalytic systems. For instance, Ru-based SILP are the result of the understanding on coordination chemistry onto Ru NPs, the effect of cations and anions of ILs in catalysis, combined with the robustness that confers the support. On that way, challenging substrates as CO_2 can be reduced with competitive activity and selectivity using Ru NPs synthesized by the organometallic approach. It is worth noting, that the reverse is also true; catalytic performances allow to understand metallic surfaces and help on the characterization of complex systems, such bimetallic NPs.

Deuteration

Isotope labelling, particularly deuteration, is an important tool for the development of new drugs, specifically for identification and quantification of metabolites. Many efficient methodologies have been developed for the synthesis of selectively deuterated compounds, including hydrogen isotope exchange (HIE).[98-100] HIE is usually performed *via* a C-H activation, which allows to introduce the deuterium into organic compounds at a late stage. Acid- or base-mediated hydrogen-deuterium exchange reactions lack of selectivity and usually need harsher conditions than metal-catalysed ones. Homogeneous phase using precious or earth abundant metals have dominated the research in this domain, due to the mild reaction conditions in which they proceed and the scope and selectivity they show. Nevertheless, heterogeneous catalysts have been described, typically based on precious metals, Pt and Pd on carbon, that provide multi H/D exchange of arenes and heterocyclic amines using

H_2/D_2O.[101] Recently, Ru[102] and Ir[103] NPs have been investigated in HIE, with promising activity. Ru/PVP NPs were efficient at H/D exchange, achieving the deuteration of pyridines, quinolines, indoles, and alkyl amines using D_2 as deuterium source under mild reaction conditions (1-2 bar of deuterium gas at room temperature or 55 °C).[102] The methodology was extended to other substrates such as amino acids and peptides,[104] and also oxazole, imidazole, triazole and carbazole substructures,[105] or oligonucleotides.[106] Since the early finding,[102] efforts have been devoted to design better deuteration nanocatalysts. Ligand effects[106-108] and the introduction of a second metal[109, 110] have been investigated. It has been demonstrated as well that Ru/C catalysts are efficient for HIE,[111] and that these supported catalysts can be modified by the introduction of an NHC, providing more selective deuteration.[112] NHCs have proved to be excellent surface modifiers of Ru NPs to provide H/D exchange. L-lysine was enantiospecifically deuterated in water using water soluble NHC-functionalized Ru NPs.[107] Oligonucleotides were also deuterated using an NHC as surface modifier, which changed the catalyst solubility, therefore, leading to an increase in the efficiency of the labelling process.[106]

The use of heterogeneous catalysis for deuteration reactions, and specifically colloidal NPs, is in its infancy. Remarkably, the works aforementioned with Ru NPs have opened the door to this field, which will probably flourish in the coming years.

Hydrogen evolution reaction

In this section, electrocatalytic and photocatalytic hydrogen evolution catalyzed by Ru NPs prepared by the organometallic approach will be described. Renewable production of hydrogen through water splitting ($2H_2O \rightarrow 2H_2 + O_2$) is a key target to reach the carbon neutral energy. One remaining challenge in this technology is to have at disposal high-performing and robust catalysts for both WS half reactions, oxygen evolution (OER) and hydrogen evolution (HER).

Electrocatalytic HER

The use of MNPs in electrocatalytic reactions is a very appealing approach, as electrodes can be easily functionalized from colloidal inks containing dispersed MNPs, by drop-casting or electrospray deposition. The use of nanoparticles as catalytic species has the benefit to expose more active sites compared to heterogeneous electrodes.

Ruthenium has demonstrated that it can be competitive *vs*. usual Platinum for the electrocatalytic HER. As a consequence, publications focusing on the use of Ru NPs for this reaction have increased exponentially,[113, 114] since 2016. In all studies described herein, [Ru(η^4-C_8H_{12})(η^6-C_8H_{10})] was used as the metal precursor, this complex easily yielding very small Ru NPs upon mild hydrogenation conditions. In all cases, a soft passivation of the Ru NPs led to a Ru/RuO_2 core/shell structure, as demonstrated by XPS or WAXS analyses.

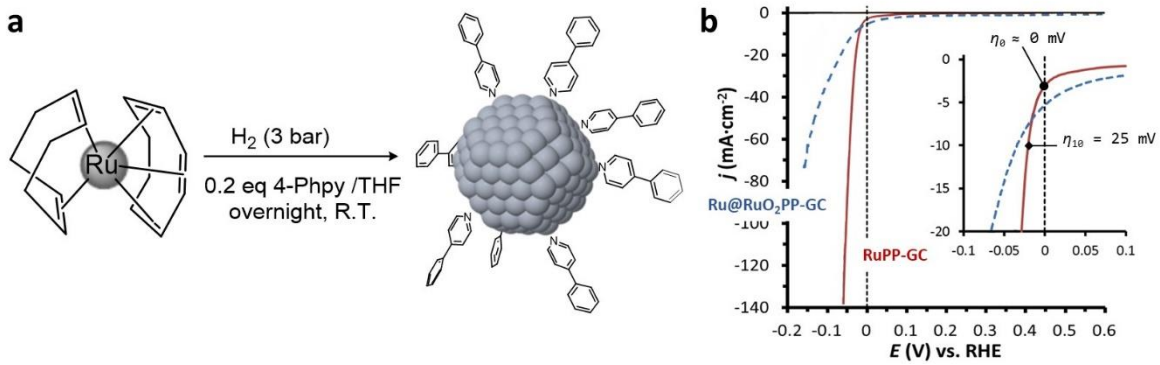

Figure 6. a) Synthesis of 4-phenylpyridine-capped Ru NPs (RuPP) by the organometallic approach. b) Linear sweep voltammetry of RuPP before (dashed line) and after (solid line) applying a reductive potential in 1M H_2SO_4. Reprinted (adapted) with permission from [113]. Copyright 2018 American Chemical Society.

To start with, 4-phenylpyridine-capped Ru NPs (RuPP) of 1.5 nm in size were found as a highly efficient electrocatalyst for HER (Figure 6 a).[115] The performance was evaluated in both 1 M H_2SO_4 and 1 M NaOH electrolytes upon deposition of the RuPP colloidal ink onto a rotating glassy carbon electrode. According to XPS, applying a reductive potential yielded a back reduction of the Ru/RuO_2 core/shell structure to pure Ru^0, keeping the ligand at the metal surface. After such an activation process, this catalyst is one of the best reported for HER. With an overpotential of η_{10} of 25 mV, TOF of 17 s^{-1} at η

= 100 mV and a stability for more than 12h at j = -10 mA·cm^{-2} it is even superior to the Pt/C reference (see Figure 6 b). These experimental observations were corroborated by DFT calculations, using as model a Ru_{55} nanocluster where the π-coordination of 4-phenylpyridine (that is preferred to σ-coordination), steric hindrance and hydrides at the Ru surface were considered. DFT-calculated dissociative adsorption Gibbs free energy ΔG_{H^*} (in kcal/mol) of some selected hydrides were found to lie on the top of the Volcano plot at 0 kcal/mol, thus indicating that the Ru-H strength is ideal to yield catalytic hydrogen evolution.[39]

One key factor to boost the performance of Ru NP-electrocatalysts is to use a support to facilitate the electron transfer between the NPs and the electrode. There is another advantage in terms of stability and dispersibility: the use of supports prevents agglomeration of the NPs under turnover conditions, thus allowing to maintain the catalytic activity over several hours without changes in the morphology of the catalyst. Carbonaceous supports are often used for this purpose.

Ru NP-modified carbon microfibers have been used as homemade working electrodes for HER.[116] Electrodes containing 0.5 wt% of Ru were prepared by two different ways: *in-situ,* by direct synthesis of the Ru NPs from [Ru(η^3-C_4H_7)$_2$(η^4-C_8H_{12})] on top of the carbon fibers and *ex-situ,* by impregnating the carbon fibers with a colloidal suspension of pre-formed RuPP NPs. Also, two types of fibers have been investigated: commercial pristine carbon fibers (pCF) and functionalized carbon fibers with carboxylic groups (fCF) obtained after an oxidation treatment. This led to four different electrodes: *in-situ* Ru@pCF and Ru@fCF, and *ex-situ* RuPP@pCF and RuPP@fCF, all presenting small Ru NPs (1.0-1.8 nm) at their surface. Evaluation of these Ru-modified carbon fibers as working electrodes for HER was performed in 1 M H_2SO_4. Different stability and activity were found, as the result of the effect of 4-PP ligand and the support on the RuNP activity. Performance of *ex-situ* materials, with overpotentials η_{10} of 225 mV for RuPP@pCF and 180 mV for RuPP@fCF was found higher than that of *in-situ* materials, highlighting a positive influence of the 4-phenylpyridine ligand on the catalytic activity of the Ru NPs, as previously observed for non-supported RuPP system. RuPP@pCF showed remarkable stability

attributed to the π-interaction between 4-phenylpyridine ligand and the pristine carbon fibers, which is disfavoured by carboxylic functional groups of fCF.

The use of alginate-derived graphenes as supports of Ru NPs for the electrocatalytic hydrogen evolution has also been studied.[117] Following *in-situ* synthesis conditions, bare graphene (G) and phosphorous-doped graphene (P-G) yielded supported Ru/RuO_2 NPs with a mean size of 1.9 nm (Ru/G) and 1.5 nm (Ru/P-G), respectively. Performances of both catalysts have been compared in 1 M H_2SO_4. Nanoparticles in Ru/G were found better dispersed than Ru/P-G. This difference is likely due to the higher exfoliation of G according to the ECSA values obtained (19.6 cm^2 for G and 3.6 cm^2 for P-G), which could provide a better performance for Ru/G material. Electrochemical activation of Ru/G and Ru/P-G by reduction of the RuO_2 layer at j = -10 $mA \cdot cm^{-2}$ ended-up with η_{10} overpotentials of 29 mV and 15 mV for the bare and P-doped electrodes, respectively. Unexpectedly given the ECSA values measured, Ru/P-G gave a higher activity than Ru/G. Therefore, the P doping of the graphene in the form of phosphates (as deduced from ^{31}P solid-state NMR data) induced an enhancement of the HER performance in terms of overpotential and current density. Both catalysts showed a faradaic efficiency of 97 and 98% and no deactivation signs upon 12h of chronopotentiometry at j = -10 $mA \cdot cm^{-2}$. Furthermore, TEM analysis indicated that the morphology of the Ru NPs was maintained in the applied HER conditions.

Photocatalytic HER

The development of photocatalysts for the HER are still in its infancy. The photocatalytic activity strongly depends on the nature of the catalyst and currently there are no efficient commercial devices able to produce hydrogen from water under sunlight activation. Two unusual examples of photocatalysts based on colloidal nanomaterials containing Ru NPs prepared by the organometallic approach have been recently reported. Note that a comparison is precluded as no benchmarking protocol to compare photocatalytic HER has been described to date.

The photocatalytic version of the HER, using as catalyst the abovementioned 4-phenylpyridine functionalized Ru nanoparticles, was achieved by depositing the RuPP NPs onto a semiconductor material (TiO_2) by a simple impregnation step, followed by the grafting of a molecular visible-light absorbent, $[Ru(bpy)_2(4,4'-(PO_3H_2)_2(bpy))]Cl_2$ complex, onto TiO_2.[118] The so-obtained hybrid nanomaterial was able to produce 417 mol H_2/mol Ru under visible light irradiation with a Xe lamp in pH 7, using triethanolamine as sacrificial electron donor. Interestingly, the photocatalytic activity could be kept for more than 90h prior to deactivation. A complete photophysical study by transient absorption spectroscopy allowed to identify the rate-determining step of the photocatalytic process. It also highlighted the two different roles of TiO_2 in the process: a role of support preventing the NP coalescence under turnover conditions, and a role of electron-transfer mediator between the RuPP NPs and the molecular photoabsorbent anchored onto the TiO_2 surface. These results differ from previous works[119] reporting that Ru NPs were poorly active or inactive for the photocatalytic HER in the presence of $[Ru(bpy)_3]^{2+}$ derivatives, because the electron-transfer mediator between the photosensitizer and the catalyst was not obvious. Only photosensitizers with long-lived excited states are able to inject electron to the catalyst, otherwise back-electron transfer processes hamper the HER.

Naked Ru NPs onto carbon nanoallotropes (CNMs) in synergy with mesoporous graphitic carbon nitride (mpg-CN) were studied in the photocatalytic HER under visible light irradiation.[120, 121] The naked Ru NPs were formed *in situ* by hydrogenation of $[Ru(\eta^3\text{-}C_4H_7)_2(\eta^4\text{-}C_8H_{12})]$ onto a carbonaceous support among four different ones tested: 0D nanohorns (CNH), 1D single walled carbon nanotubes (CNT), 2D reduced graphene oxide (rGO) and 3D graphite (GP). The so-obtained Ru-based carbon materials (Ru NPs@CNMs) were then physically mixed with mpg-CN at different ratios. Ru NPs were also directly synthetized onto mpg-CN (leading to Ru NPs@mgp-CN) for comparison purpose. Dispersions of all these materials were prepared in aqueous triethanolamine solution before exposure to visible light, all of them evolving hydrogen under the stated conditions. Ru NPs@mgp-CN showed less hydrogen production than any Ru NPs@CNMs/mgp-CN (137 $\mu mol \cdot h^{-1} \cdot g^{-1}$ *vs.* 197 $\mu mol \cdot h^{-1} \cdot g^{-1}$ for Ru NPs@CNT/mgp-CN), even when incorporating 4-phenylpyridine ligand during the synthesis to boost

the activity of the nanoparticles (155 $\mu mol \cdot h^{-1} \cdot g^{-1}$). These results indicate that the CNMs play a key role on the electron-transfer processes that can be ascribed to their electrical conductivity properties. Although all materials are excellent supports for Ru NPs, with large surface areas and easy versatility, the observed differences in photocatalytic activity are not significant enough to have pertinent conclusions about the support effect. On the other side, analysis of the different ratios of Ru NPs@CNMs onto mgp-CN resumed in finding two competitive effects during the photocatalytic process. If at a higher ratio of Ru NPs one can expect to have a higher catalytic activity as the result of more Ru active sites present, it can be also expected that less light will be absorbed by mpg-CN due to the coverage by the Ru NPs. This was confirmed as a higher amount of H_2 was evolved at higher %Ru but higher TON was achieved for the lower metal loading. Remarkably, these materials also showed high stability under the applied photocatalytic conditions, with no sign of deactivation over 75h.

Ru NPs synthesized by the organometallic approach provided pertinent catalytic systems to replace Pt for the electrocatalytic and photocatalytic HER. The presented case studies concern Ru NPs stabilized by an organic ligand, a carbonaceous support or both. The ligand and support were shown to be key factors to access highly performant catalysts. Some of the examples described display superior activity than commercial Pt/C, the RuPP electrocatalyst being among the state-of-the-art catalysts for the HER. In order to precisely understand the role of the ligand, comparison studies using other ligand-capped Ru NPs need to be performed. Combining electrochemical performance, characterization data by complementary analytical techniques together with computational modelling should help to rationalize the ligand effect and define the most appropriate ones for a performant HER. Choosing a support can be crucial for the performance as it can improve the stabilization of the NPs by avoiding aggregation and also enhancing the electron transfer processes. If the field is in exponential development, the design of functional cells to produce low-priced green hydrogen by electrocatalytic HER still needs further development of catalysts in terms of efficiency and roughness. This is even more right for photocatalytic HER, a domain that is only at its infancy. To sum up the results described above evidence the interest of the organometallic approach to develop performant Ru-based electrocatalysts

and photocatalysts for HER, even if the size effect remains unexplored. The same synthesis approach can be followed to develop also electrocatalysts for OER.[122]

Miscellaneous reactions

This section presents other organic transformations for which Ru NPs synthesized by the organometallic approach have been implemented as catalysts.

Aerobic oxidation of hydrocarbons is a common green route to avoid highly pollutant oxidants. The main obstacle to overcome during aerobic oxidation is the lack of selectivity, linked to the harsh conditions, that often leads to mixture of products including alcohols, ketones, epoxides, aldehydes or carboxylic acids. Recently, one example of solvent-free oxidation of cyclic alkenes by Ru NPs stabilized by ionic liquids has been described. Ru NPs functionalized by BMIm.BF4 (ca. 1-2 nm in size) deposited onto morphologically different TiO_2 supports (nanoparticles, nanotubes and nanofibers) have been shown of interest for the oxidation of cyclohexene and 2,3-dihydro-1H-inden-1-one.[123] Among the different nanomaterials tested, Ru NPs supported onto TiO_2 nanofibers (Ru/TiO_2NFs) showed the best efficiencies. In comparison, Ru/TiO_2 nanoparticles and Ru/TiO_2 nanotubes showed only 92 and 84% conversion, respectively. The Ru/TiO_2NFs catalyst also provided 95% conversion in the allylic oxidation of cyclohexene, with 78% selectivity towards 2-cyclohexen-1-one at 75°C under 4 bar of O_2. In the allylic oxidation of indane, it also achieved 70% conversion with 85% selectivity towards 1-indanone. The high performance observed with Ru/TiO_2NFs is supposed to be related to the surface morphology, pore size and surface area of the support. The catalyst was found recyclable for 5 runs. This example paves the wave for industrial compounds green oxidation.

Ru NPs prepared by hydrogenation of $[Ru(\eta^4\text{-}C_8H_{12})(\eta^6\text{-}C_8H_{10})]$ in the presence of SNS tridentate pincer-type ligands have been found to efficiently catalyze the reduction of the greenhouse gas N_2O into N_2.[124] Reaction conditions applied comprise the use of different hydrosilanes as reductant and mild reaction

conditions (1 bar N_2O, 55–65 °C) (Figure 7). This also provided potentially useful Si–O containing derivatives as the result of the oxidation of the silanes.

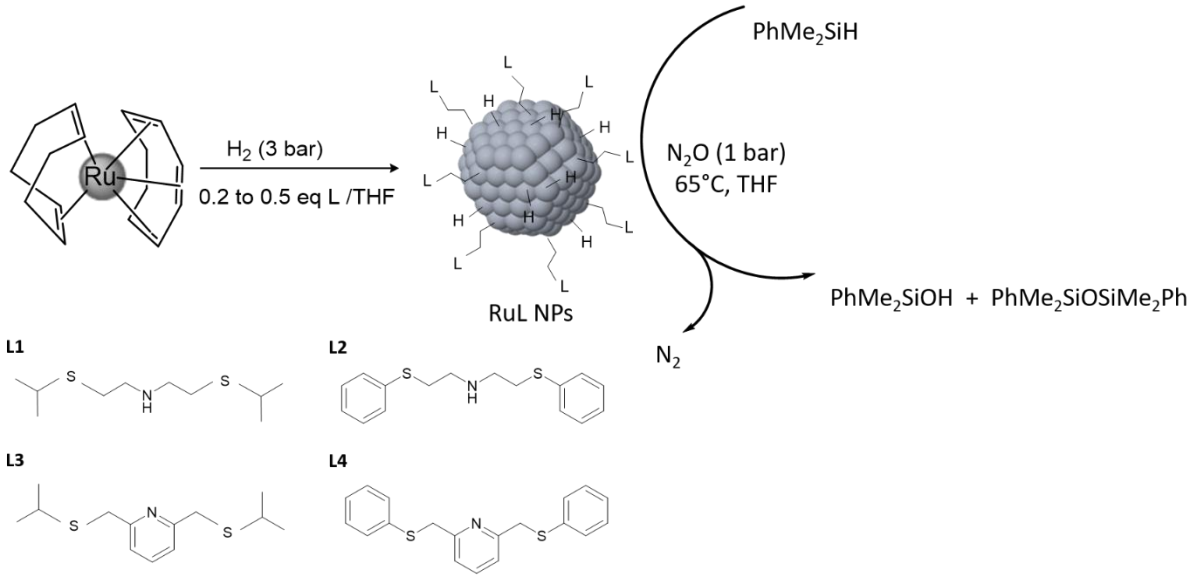

Figure 7. Reduction of N_2O on Ru/SNS ligands using silanes.

A multifunctional nanomaterial composed of a silica support covalently functionalized by copper N-heterocyclic carbene (NHC) complexes and Ru NPs, Ru NPs@SiO_2-[Cu-NHC], was found active and selective for the one-pot two-step catalytic synthesis of a wide range of allylamines and alkylamines, that are important products in the fine chemical and pharmaceutical industry.[125] The molecular approach followed to prepare this material consisted in two steps. The Ru NPs were formed *in situ* by hydrogenation of [Ru(η^3-C_4H_7)$_2$(η^4-C_8H_{12})] previously impregnated onto the SiO_2 support. Then, the the (1-butyl-3-(3-(triethoxysilyl)propyl)-2,3-dihydro-1H-imidazol-2-yl)copper(I) chloride complex, [Cu-NHC], was covalently chemisorbed onto Ru NPs@SiO_2 by a silanization procedure. Deep analytical investigation (HRTEM, STEM-HAADF, NMR, XPS, etc.) evidenced that the immobilized molecular [Cu–NHC] complex was responsible for the atom-efficient A3 coupling of amines, formaldehyde, and terminal alkynes, while the selective hydrogenation of the resulting propargyl amines was catalyzed by Ru NPs. Catalyst activity and selectivity remained fairly constant for three catalytic cycles, with a slight decrease in hydrogenation activity with time. This innovative Ru-based nanomaterial highlights a new generation of nanoparticles immobilized onto a molecularly modified support which, in the

reported work, significantly reduced the number of side reactions, separation, and purification steps usually required in conventional multistep approaches. This work opens the way to the development of multifunctional catalytic systems capable of performing complex reaction sequences in one pot conditions.

Formic acid (FA) can be obtained by the hydrothermal conversion of CO with H_2O, but this reaction usually requires very high pressures (>100 bar) and temperatures (>200°C) and days to complete. The formation of formic acid by a catalytic semi-water-gas shift reaction (SWGSR) in mild conditions using supported RuFe NPs embedded in an ionic liquid (IL)-hybrid silica as catalyst has been reported.[126] Two nanomaterials were prepared following a two-step procedure. First, a reduction/decomposition of $[Ru(\eta^3\text{-}C_4H_7)_2(\eta^4\text{-}C_8H_{12})]$ and $Fe(CO)_5$ complexes under H_2 atmosphere was performed in BMIm·as solvent and stabilizer. Then, the RuFe NPs were embedded into an IL-hybrid silica (SILP-OAc or SILP-NTf_2) following the method presented in Figure 4, leading to RuFeNPs@SILP of ca. 1.0 nm in size in SILP-NTf_2 and ca. 2.1 nm in SILP-OAc. The smaller size of NPs observed on the SILP-NTf_2 support derives from its hydrophobic nature and weak cation–anion interaction strength (Im–NTf_2), which prevents the aggregation of RuFe NPs. The larger NP size obtained with the SILP-OAc support can be explained by an hydrophilic effect and strong cation–anion interaction strength (Im–OAc) that may cause aggregation. The location of the alloy RuFe NPs on the silica was also found to strongly depends on the nature of the anion. With hydrophilic SILP-OAc, RuFe NPs were more exposed to the support surface than with the hydrophobic SILP-NTf_2 support. However, a higher catalytic activity was obtained using the hydrophobic support. The RuFe NPs in the SILP-NTf_2 were found to be very active for the selective conversion of CO to free FA, in an aqueous solution of imidazolium-based IL and under mild conditions (10 bar CO and 80°C), with a turnover number of up to 1269. In a comparison study with monometallic systems prepared in same conditions, no FA was detected on FeNPs@SILP-NTf_2 catalyst but FA was formed in a significant amount (turnover number of 174) on the Ru@SILP-NTf_2 one. This work clearly showed that the combination of Ru with Fe into the RuFe@SILP-NTf_2 nanomaterial led to a significantly increased activity for the selective production of FA as the result of the dominance of SWGSR thanks

to a positive metal dilution effect. The Fe/SILP-NTf_2 system can be seen as a catalytic membrane, controlling the access and local concentration of the reactants/products to the active site and expelling the free FA to the aqueous phase. This work proposes a promising alternative for the production of free FA, in which the water is the hydrogen source, as opposed to the direct hydrogenation of CO_2.

The implementation of Ru NPs was shown to be also advantageous in a few reactions for which they are not usually applied. The results obtained with TiO_2-supported Ru NPs in aerobic oxidation of hydrocarbons showed high efficiencies in mild conditions and revealed an effect of the morphology, pore size and surface area of the support on the catalytic performance. The combination of Ru/SNS NPs with silanes led to the reduction of NO_2 to N_2 while furnishing Si-O compounds, highlighting a double interest of the procedure applied. A hybrid catalyst, RuFe NPs-imidazolium-based IL- silica, gave rise to the selective production of formic acid by carbonylation of water, in an aqueous solution of IL and under mild reaction conditions. In this study, besides a synergy between the two metals, the hydrophobicity of the IL appeared to be a key-parameter for the catalytic semi-water-gas shift reaction. All these results highlight the interest of Ru NPs for other types of reactions than traditional hydroconversion catalysis, as also described above for deuteration and hydrogen evolution reactions.

Conclusions and perspectives

In this chapter we have reported on the recent advances in the investigation of catalytic properties of Ru NPs synthesized *via* the organometallic approach. In the last years, hydroconversion catalysis was the most studied topic using this type Ru NPs that are reputed to display very small sizes, narrow size distributions as well as well-defined compositions and structural features. The hydroconversion section describes the catalytic transformation of different families of substrates for the production of compounds that present an industrial interest for applications in the domains of fine chemistry or fuels. The results show that Ru NPs display high performances in hydrogenation and dehydrogenation reactions of compounds that contain alkynyl, olefinic or carbonyl groups. The common objectives in

the reported studies were to find appropriate reaction conditions in order to achieve high selectivity while keeping efficient reactivity at mildest temperature and hydrogen pressure as possible, for green and cost concerns, and the Ru tested NPs proved to be pertinent systems to achieve the target compounds. Another interest of the described works is the coupling of experimental results and theoretical realistic views of the nanocatalysts. Comparatively to the areas of homogeneous and heterogeneous catalysis, such a strategy is quite recent in nanocatalysis but it progressed in the last years. This development relies on the use of powerful computational tools that permit to determine the surface state and the surface reactivity of metal nanoparticles on the basis of precisely defined model systems that mimic well the nanoparticles investigated in catalysis. The understanding of the coordination of ligands and substrates at the NP surface, or that of the addition of a second metal, provided pivotal information on the catalytic behaviour of Ru NP systems. Also, the use of supports like ILs or of SILPs conditions, that are known to provide robust catalytic systems, allowed to achieve specific and performant Ru-based catalytic systems for hydrogenation catalysis. Thus, reduction of CO_2 was shown feasible using as catalyst SILP-supported Ru NPs synthesised by the organometallic approach with competitive activity and selectivity. Knowing that the reduction of CO2 is a challenging reaction for which only a few heterogeneous catalysts have been described in the literature and not Ru-based although this metal is highly performant in homogenous catalysis, this result is promising.

Electrocatalytic hydrogen evolution is another application for which Ru NPs have been investigated in the last years, which led to the rebirth of Ru for this challenging reaction. Aiming at producing hydrogen -usable as a fuel or energy vector- through the splitting of water molecules, HER is seen as a promising alternative to the consumption of fossil fuels. Ru NPs synthesized by the organometallic approach provided competitive catalytic systems to classical Pt catalysts. Studies of the effect of stabilizing ligands and functionalized-carbonaceous supports indicated they are key factors to achieve performant catalysts. Today, the phenylpyridine-stabilized NPs above mentioned count among the state-of-the-art catalysts for HER. However, there is a lack of comparative studies on ligand-capped and supported-Ru NPs, thus precluding a comprehensive rationalization of ligand and support effects.

This needs to be performed in order to accurate their role onto the electrocatalytic mechanism and also stability of the NPs in reaction conditions, another key feature before envisaging applications. Collect electrochemical and analytical characterization data -including in *operando* conditions- together with computational studies, should contribute to the design of appropriate catalysts for a performant and durable HER. If the electrocatalytic HER is an attractive solution to face energy concerns, the design of cells to access hydrogen, in an efficient but inexpensive way, requires to have competitive and robust catalysts compared to Pt ones used presently in electrolizers. Light-driven HER studies have been also investigated with Ru NP-based catalytic systems derived from the organometallic approach. For this purpose, the Ru NPs were associated with a photoabsorbant and a conducting material, that led also to interesting perspectives. However, more work is needed in order to improve and control the electron exchanges that are at the basis of this nature-inspired concept. To sum up the interest of the organometallic approach to develop performant Ru-based electrocatalysts and photocatalysts for HER has been evidenced, with pertinent results on the influence of ligands and supports, but the study of the NP size effect remains unexplored.

The implementation of Ru NPs was shown to be also advantageous in a few reactions for which they are not usually applied. The deuteration reaction using D_2 or D_2O as the source of deuterium is a valuable application as it allows to access deuterated compounds that are of pharmaceutical or biological interest. The use of heterogeneous catalysts for this reaction is quite rare, and more specifically concerning colloidal NPs. The remarkable results obtained with Ru NPs in mild reaction conditions should attract more research efforts in this field in the near future, pushed by the industrial needs. Ru NPs were also reported as active catalysts for the aerobic oxidation of hydrocarbons with high efficiencies in mild conditions. The reduction of NO_2 to N_2 with the subsequent formation of Si-O compounds, as the result of the oxidation of the silanes used as reductants, also illustrates well the potential of Ru nanocatalysts for green oxidation reactions in mild conditions. The last example concerns the use of an hybrid RuFe NPs-imidazolium-based IL-silica catalytic system, that allowed the selective production of formic acid by carbonylation of water, in aqueous and mild reaction conditions.

In this catalytic semi-water-gas shift reaction, synergy effects between the two metals have been evidenced, together with that of the hydrophobicity of the IL on the catalysis results. The different works described in the last section of this chapter emphasize the catalytic performances of Ru NPs in non-typical reactions compared to hydroconversion catalysis for which ruthenium-based systems are already recognized. This may derive from the knowledge acquired from the implementation of Ru NPs in hydrogenation or hydrogenolysis catalysis, that may render them attractive to achieve other catalysis objectives.

It is worth to note that nanoparticles of other metals than ruthenium and prepared by the organometallic strategy, have been also published by different research groups from academia sector, interested in having well-defined MNPs for studying structure/properties correlations in catalysis. The surface chemistry of MNP is nowadays better understood, not only because of the compilation of numerous experimental data but also that of computational ones. If the combination of experimental and theoretical results was shown to be a success for the design of more performant catalytic systems the reverse is also true. Probing catalytic performances is also a pertinent way to understand metallic surfaces and complete the characterization of complex systems, such as bimetallic NPs. The recent advances provide a solid basis to investigate new catalytic processes on the metal surface and explore how these can be affected by the stabilizing molecules and/or supports. We believe that inspiration taken from the concepts of the different fields of catalysis (homogeneous, heterogeneous and enzymatic) will contribute to the development of highly performant nanocatalysts and stable enough to be recycled at long operating period of time without loss of activity/selectivity. This is a prerequisite to a greener catalysis, and to contribute to the challenges our modern society face in terms of environment, energy and economy.

Acknowledgement

Authors thank CNRS and Université de Toulouse - Paul Sabatier for funding.

References

(1) Jin, R.; Zeng, C.; Zhou, M.; Chen, Y. Atomically precise colloidal metal nanoclusters and nanoparticles: Fundamentals and opportunities. *Chem. Rev.* **2016**, *116* (18), 10346-10413. DOI: 10.1021/acs.chemrev.5b00703.

(2) Jin, R.; Pei, Y.; Tsukuda, T. Controlling nanoparticles with atomic precision. *Acc. Chem. Res.* **2019**, *52* (1), 1. DOI: 10.1021/acs.accounts.8b00631.

(3) Astruc, D. Introduction: Nanoparticles in catalysis. *Chem. Rev.* **2020**, *120* (2), 461-463. DOI: 10.1021/acs.chemrev.8b00696.

(4) Schmid, G. *Nanoparticles: From theory to application*; Wiley-Blackwell, 2010.

(5) Astruc, D.; Editor. *Nanoparticles and catalysis*; Wiley-VCH Verlag GmbH & Co. KGaA, 2008.

(6) Kaatz, F. H.; Bultheel, A. Magic mathematical relationships for nanoclusters. *Nanoscale Res. Lett.* **2019**, *14* (1), 1-12. DOI: 10.1186/s11671-019-2939-5.

(7) Shi, Y.; Lyu, Z.; Zhao, M.; Chen, R.; Nguyen, Q. N.; Xia, Y. Noble-metal nanocrystals with controlled shapes for catalytic and electrocatalytic applications. *Chem. Rev.* **2021**, *121* (2), 649-735. DOI: 10.1021/acs.chemrev.0c00454.

(8) Ubasart, E.; Mustieles Marin, I.; Asensio, J. M.; Mencia, G.; Lopez-Vinasco, A. M.; Garcia-Simon, C.; del Rosal, I.; Poteau, R.; Chaudret, B.; Ribas, X. Supramolecular nanocapsules as two-fold stabilizers of outer-cavity sub-nanometric Ru NPs and inner-cavity ultra-small Ru clusters. *Nanoscale Horiz.* **2022**, *7* (6), 607-615. DOI: 10.1039/d1nh00677k.

(9) Luo, Y.; Wu, Y. Defect engineering of nanomaterials for catalysis. *Nanomaterials* **2023**, *13* (6), 1116. DOI: 10.3390/nano13061116.

(10) Axet, M. R.; Philippot, K. Chapter 4 - Organometallic metal nanoparticles for catalysis. In *Nanoparticles in catalysis*, Philippot, K., Roucoux, A. Eds.; Wiley, 2021; pp 73-97.

(11) Tan, L.-L.; Wei, M.; Shang, L.; Yang, Y.-W. Cucurbiturils-mediated noble metal nanoparticles for applications in sensing, SERS, theranostics, and catalysis. *Adv. Funct. Mater.* **2021**, *31* (1), 2007277. DOI: 10.1002/adfm.202007277.

(12) Bordet, A.; Leitner, W. Metal nanoparticles immobilized on molecularly modified surfaces: Versatile catalytic systems for controlled hydrogenation and hydrogenolysis. *Acc. Chem. Res.* **2021**, *54* (9), 2144-2157. DOI: 10.1021/acs.accounts.1c00013.

(13) Mustieles Marin, I.; Asensio, J. M.; Chaudret, B. Bimetallic nanoparticles associating noble metals and first-row transition metals in catalysis. *ACS Nano* **2021**, *15* (3), 3550-3556. DOI: 10.1021/acsnano.0c09744.

(14) Serp, P.; Philippot, K.; Editors. *Nanomaterials in catalysis*; 2013. DOI: 10.1002/9783527656875.

(15) Philippot, K.; Roucoux, A.; Editors. *Nanoparticles in catalysis: Advances in synthesis and applications*; Wiley-VCH Weinheim, 2021.

(16) Roucoux, A.; Philippot, K. New trends in the design of metal nanoparticles and derived nanomaterials for catalysis. In *Nanoparticles in catalysis: Advances in synthesis and applications*, Philippot, K., Roucoux, A. Eds.; Wiley-VCH Weinheim, 2021; pp 1-11.

(17) Lu, L.; Zou, S.; Fang, B. The critical impacts of ligands on heterogeneous nanocatalysis: a review. *ACS Catal.* **2021**, *11* (10), 6020-6058. DOI: 10.1021/acscatal.1c00903.

(18) Asensio, J. M.; Bouzouita, D.; van Leeuwen, P. W. N. M.; Chaudret, B. σ-H-H, σ-C-H, and σ-Si-H bond activation catalyzed by metal nanoparticles. *Chem. Rev.* **2020**, *120* (2), 1042-1084. DOI: 10.1021/acs.chemrev.9b00368.

(19) Zhukhovitskiy, A. V.; MacLeod, M. J.; Johnson, J. A. Carbene ligands in surface chemistry: From stabilization of discrete elemental allotropes to modification of nanoscale and bulk substrates. *Chem. Rev.* **2015**, *115* (20), 11503-11532. DOI: 10.1021/acs.chemrev.5b00220.

(20) Heuer-Jungemann, A.; Feliu, N.; Bakaimi, I.; Hamaly, M.; Alkilany, A.; Chakraborty, I.; Masood, A.; Casula, M. F.; Kostopoulou, A.; Oh, E.; et al. The role of ligands in the chemical synthesis and applications of inorganic nanoparticles. *Chem. Rev.* **2019**, *119* (8), 4819-4880. DOI: 10.1021/acs.chemrev.8b00733.

(21) Boles, M. A.; Ling, D.; Hyeon, T.; Talapin, D. V. The surface science of nanocrystals. *Nat. Mater.* **2016**, *15* (2), 141-153. DOI: 10.1038/nmat4526.

(22) Amiens, C.; Chaudret, B.; Ciuculescu-Pradines, D.; Colliere, V.; Fajerwerg, K.; Fau, P.; Kahn, M.; Maisonnat, A.; Soulantica, K.; Philippot, K. Organometallic approach for the synthesis of nanostructures. *New J. Chem.* **2013**, *37*, 3374-3401. DOI: 10.1039/c3nj00650f.

(23) Amiens, C.; Ciuculescu-Pradines, D.; Philippot, K. Controlled metal nanostructures: Fertile ground for coordination chemists. *Coord. Chem. Rev.* **2016**, *308*, 409-432. DOI: 10.1016/j.ccr.2015.07.013.

(24) Reina, A.; Favier, I.; Pradel, C.; Gomez, M. Stable zero-valent nickel nanoparticles in glycerol: Synthesis and applications in selective hydrogenations. *Adv. Synth. Catal.* **2018**, *360* (18), 3544-3552. DOI: 10.1002/adsc.201800786.

(25) Favier, I.; Pla, D.; Gomez, M. Palladium nanoparticles in polyols: Synthesis, catalytic couplings, and hydrogenations. *Chem. Rev.* **2020**, *120* (2), 1146-1183. DOI: 10.1021/acs.chemrev.9b00204.

(26) Min, Y.; Nasrallah, H.; Poinsot, D.; Lecante, P.; Tison, Y.; Martinez, H.; Roblin, P.; Falqui, A.; Poteau, R.; del Rosal, I.; et al. 3D Ruthenium nanoparticle covalent assemblies from polymantane ligands for confined catalysis. *Chem. Mater.* **2020**, *32* (6), 2365–2378. DOI: 10.1021/acs.chemmater.9b04737.

(27) Gonzalez-Gomez, R.; Cusinato, L.; Bijani, C.; Coppel, Y.; Lecante, P.; Amiens, C.; del Rosal, I.; Philippot, K.; Poteau, R. Carboxylic acid-capped ruthenium nanoparticles: experimental and theoretical case study with ethanoic acid. *Nanoscale* **2019**, *11* (19), 9392-9409. DOI: 10.1039/c9nr00391f.

(28) Lara, P.; Philippot, K.; Suarez, A. Phosphane-decorated platinum nanoparticles as efficient catalysts for H_2 generation from ammonia borane and methanol. *ChemCatChem* **2019**, *11* (2), 766-771. DOI: 10.1002/cctc.201801702.

(29) Cerezo-Navarrete, C.; Lara, P.; Martinez-Prieto, L. M. Organometallic nanoparticles ligated by NHCs: Synthesis, surface chemistry and ligand effects. *Catalysts* **2020**, *10* (10), 1144. DOI: 10.3390/catal10101144.

(30) Cardona-Farreny, M.; Lecante, P.; Esvan, J.; Dinoi, C.; Del Rosal, I.; Poteau, R.; Philippot, K.; Axet, M. R. Bimetallic RuNi nanoparticles as catalysts for upgrading biomass: metal dilution and solvent effects on selectivity shifts. *Green Chem.* **2021**, *23*, 8480-8500. DOI: 10.1039/D1GC02154K.

(31) Garg, G.; Foltran, S.; Favier, I.; Pla, D.; Medina-Gonzalez, Y.; Gomez, M. Palladium nanoparticles stabilized by novel choline-based ionic liquids in glycerol applied in hydrogenation reactions. *Catal. Today* **2020**, *346*, 69-75. DOI: 10.1016/j.cattod.2019.01.052.

(32) Martin Morales, E.; Coppel, Y.; Lecante, P.; del Rosal, I.; Poteau, R.; Esvan, J.; Sutra, P.; Philippot, K.; Igau, A. When organophosphorus ruthenium complexes covalently bind to ruthenium nanoparticles to form nanoscale hybrid materials. *Chem. Commun.* **2020**, *56* (29), 4059-4062. DOI: 10.1039/d0cc00442a.

(33) Axet, M. R.; Philippot, K. Catalysis with colloidal ruthenium nanoparticles. *Chem. Rev.* **2020**, *120*, 1085-1145. DOI: 10.1021/acs.chemrev.9b00434.

(34) Martinez-Prieto, L. M.; Chaudret, B. Organometallic ruthenium nanoparticles: synthesis, surface chemistry, and insights into ligand coordination. *Acc. Chem. Res.* **2018**, *51*, 376-384. DOI: 10.1021/acs.accounts.7b00378.

(35) Ramamoorthy, R. K.; Soulantica, K.; Del Rosal, I.; Arenal, R.; Decorse, P.; Piquemal, J.-Y.; Chaudret, B.; Poteau, R.; Viau, G. Ruthenium icosahedra and ultrathin platelets: The role of surface chemistry on the nanoparticle structure. *Chem. Mater.* **2022**, *34* (7), 2931-2944. DOI: 10.1021/acs.chemmater.1c03452.

(36) Gonzalez Gomez, R.; del Rosal, I.; Philippot, K.; Poteau, R. DFT calculations in periodic boundary conditions of gas-phase acidities and of transition-metal anionic clusters: case study with carboxylate-stabilized ruthenium clusters. *Theor. Chem. Acc.* **2019**, *138* (8), 1-10. DOI: 10.1007/s00214-019-2484-4.

(37) Foppa, L.; Yamamoto, K.; Liao, W.-C.; Comas-Vives, A.; Coperet, C. Electronic structure-reactivity relationship on ruthenium step-edge sites from carbonyl ^{13}C chemical shift analysis. *J. Phys. Chem. Lett.* **2018**, *9* (12), 3348-3353. DOI: 10.1021/acs.jpclett.8b01332.

(38) Rothermel, N.; Limbach, H.-H.; del Rosal, I.; Poteau, R.; Mencia, G.; Chaudret, B.; Buntkowsky, G.; Gutmann, T. Surface reactions of ammonia on ruthenium nanoparticles revealed by ^{15}N and ^{13}C solid-state NMR. *Catal. Sci. Technol.* **2021**, *11* (13), 4509-4520. DOI: 10.1039/d0cy02476g.

(39) del Rosal, I.; Poteau, R. Sabatier principle and surface properties of small ruthenium nanoparticles and clusters: case studies. In *Nanoparticles in catalysis*, Philippot, K., Roucoux, A. Eds.; 2021; pp 331-351.

(40) Vignolle, J.; Tilley, T. D. N-Heterocyclic carbene-stabilized gold nanoparticles and their assembly into 3D superlattices. *Chem. Commun.* **2009**, (46), 7230-7232. DOI: 10.1039/b913884f.

(41) Lara, P.; Rivada-Wheelaghan, O.; Conejero, S.; Poteau, R.; Philippot, K.; Chaudret, B. Ruthenium nanoparticles stabilized by N-heterocyclic carbenes: ligand location and influence on reactivity. *Angew. Chem., Int. Ed.* **2011**, *50*, 12080-12084, 10.1002/anie.201106348. DOI: 10.1002/anie.201106348.

(42) Rodriguez-Castillo, M.; Lugo-Preciado, G.; Laurencin, D.; Tielens, F.; van der Lee, A.; Clement, S.; Guari, Y.; Lopez-de-Luzuriaga, J. M.; Monge, M.; Remacle, F.; et al. Experimental and theoretical study of the reactivity of gold nanoparticles towards benzimidazole-2-ylidene ligands. *Chem. - Eur. J.* **2016**, *22* (30), 10446-10458. DOI: 10.1002/chem.201601253.

(43) Lara, P.; Martinez-Prieto, L. M.; Rosello-Merino, M.; Richter, C.; Glorius, F.; Conejero, S.; Philippot, K.; Chaudret, B. NHC-stabilized Ru nanoparticles: Synthesis and surface studies. *Nano-Struct. Nano-Objects* **2016**, *6*, 39-45. DOI: 10.1016/j.nanoso.2016.03.003.

(44) Martinez-Prieto, L. M.; Ferry, A.; Lara, P.; Richter, C.; Philippot, K.; Glorius, F.; Chaudret, B. New route to stabilize ruthenium nanoparticles with non-isolable chiral N-heterocyclic carbenes. *Chem. - Eur. J.* **2015**, *21*, 17495-17502. DOI: 10.1002/chem.201502601.

(45) Rakers, L.; Martinez-Prieto, L. M.; Lopez-Vinasco, A. M.; Philippot, K.; van Leeuwen, P. W. N. M.; Chaudret, B.; Glorius, F. Ruthenium nanoparticles ligated by cholesterol-derived NHCs and their application in the hydrogenation of arenes. *Chem. Commun.* **2018**, *54*, 7070-7073. DOI: 10.1039/c8cc02833h.

(46) Martinez-Prieto, L. M.; Ferry, A.; Rakers, L.; Richter, C.; Lecante, P.; Philippot, K.; Chaudret, B.; Glorius, F. Long-chain NHC-stabilized Ru NPs as versatile catalysts for one-pot oxidation/hydrogenation reactions. *Chem. Commun.* **2016**, *52*, 4768-4771. DOI: 10.1039/c6cc01130f.

(47) Bruna, L.; Cardona-Farreny, M.; Colliere, V.; Philippot, K.; Axet, M. R. In situ ruthenium catalyst modification for the conversion of furfural to 1,2-pentanediol. *Nanomaterials* **2022**, *12* (3), 328.

(48) Asensio, J. M.; Miguel, A. B.; Fazzini, P.-F.; van Leeuwen, P. W. N. M.; Chaudret, B. Hydrodeoxygenation using magnetic induction: High-temperature heterogeneous catalysis in solution. *Angew. Chem., Int. Ed.* **2019**, *58* (33), 11306-11310. DOI: 10.1002/anie.201904366.

(49) Meffre, A.; Mehdaoui, B.; Kelsen, V.; Fazzini, P. F.; Carrey, J.; Lachaize, S.; Respaud, M.; Chaudret, B. A simple chemical route toward monodisperse iron carbide nanoparticles displaying tunable magnetic and unprecedented hyperthermia properties. *Nano Lett.* **2012**, *12* (9), 4722-4728. DOI: 10.1021/nl302160d.

(50) Leng, F.; Gerber, I. C.; Lecante, P.; Moldovan, S.; Girleanu, M.; Axet, M. R.; Serp, P. Controlled and chemoselective hydrogenation of nitrobenzene over Ru@C_{60} catalysts. *ACS Catal.* **2016**, *6*, 6018-6024. DOI: 10.1021/acscatal.6b01429.

(51) Leng, F.; Gerber, I. C.; Lecante, P.; Bacsa, W.; Miller, J.; Gallagher, J. R.; Moldovan, S.; Girleanu, M.; Axet, M. R.; Serp, P. Synthesis and structure of ruthenium-fullerides. *RSC Adv.* **2016**, *6* (73), 69135-69148. DOI: 10.1039/c6ra12023g.

(52) Bouju, X.; Duguet, É.; Gauffre, F.; Henry, C. R.; Kahn, M. L.; Mélinon, P.; Ravaine, S. Nonisotropic self-assembly of nanoparticles: from compact packing to functional aggregates. *Adv. Mater.* **2018**, *30* (27), 1706558. DOI: 10.1002/adma.201706558.

(53) Neouze, M.-A. Nanoparticle assemblies: main synthesis pathways and brief overview on some important applications. *J. Mater. Sci.* **2013**, *48*, 7321-7349. DOI: 10.1007/s10853-013-7542-z.

(54) Henry, C. R. 2D-Arrays of nanoparticles as model catalysts. *Catal. Lett.* **2015**, *145*, 731–749. DOI: 10.1007/s10562-014-1402-6.

(55) Min, Y.; Axet, M. R.; Serp, P. Covalent assemblies of metal nanoparticles-strategies for synthesis and catalytic applications. In *Recent advances in nanoparticle catalysis. Molecular catalysis, vol 1.*, van Leeuwen, P., Claver, C. Eds.; Springer, Cham., 2020.

(56) Leng, F.; Gerber, I. C.; Axet, M. R.; Serp, P. Selectivity shifts in hydrogenation of cinnamaldehyde on electron-deficient ruthenium nanoparticles. *C. R. Chim.* **2018**, *21*, 346-353. DOI: 10.1016/j.crci.2017.04.001.

(57) Luo, Z.; Min, Y.; Nechiyil, D.; Bacsa, W.; Tison, Y.; Martinez, H.; Lecante, P.; Gerber, I. C.; Serp, P.; Axet, M. R. Chemoselective reduction of quinoline over Rh-C_{60} nanocatalysts. *Catal. Sci. Technol.* **2019**, *9*, 6884-6898. DOI: 10.1039/c9cy02025j.

(58) Leng, F.; Gerber, I. C.; Lecante, P.; Bentaleb, A.; Munoz, A.; Illescas, B. M.; Martin, N.; Melinte, G.; Ersen, O.; Martinez, H.; et al. Hexakis [60]fullerene adduct-mediated covalent assembly of ruthenium nanoparticles and their catalytic properties. *Chem. - Eur. J.* **2017**, *23*, 13379-13386. DOI: 10.1002/chem.201701043.

(59) Machado, B. F.; Oubenali, M.; Axet, M. R.; NGuyen, T. T.; Tunckol, M.; Girleanu, M.; Ersen, O.; Gerber, I. C.; Serp, P. Understanding the surface chemistry of carbon nanotubes: toward a rational design of Ru nanocatalysts. *J. Catal.* **2014**, *309*, 185-198. DOI: 10.1016/j.jcat.2013.09.016.

(60) Min, Y.; Leng, F.; Machado, B. F.; Lecante, P.; Roblin, P.; Martinez, H.; Theussl, T.; Casu, A.; Falqui, A.; Barcenilla, M.; et al. 2D and 3D ruthenium nanoparticle covalent assemblies for phenyl acetylene hydrogenation. *Eur. J. Inorg. Chem.* **2020**, *2020* (43), 4069-4082. DOI: 10.1002/ejic.202000698.

(61) Dupont, J.; Scholten, J. D. On the structural and surface properties of transition-metal nanoparticles in ionic liquids. *Chem. Soc. Rev.* **2010**, *39* (5), 1780-1804. DOI: 10.1039/b822551f.

(62) Qadir, M. I.; Simon, N. M.; Dupont, J. Catalytic properties of metal nanoparticles confined in ionic liquids. In *Nanoparticles in catalysis*, Philippot, K., Roucoux, A. Eds.; Wiley-VCH, GmbH Weinheim, Germany, 2021; pp 123-138.

(63) Dupont, J.; Fonseca, G. S.; Umpierre, A. P.; Fichtner, P. F. P.; Teixeira, S. R. Transition-metal nanoparticles in imidazolium ionic liquids: recyclable catalysts for biphasic hydrogenation reactions. *J. Am. Chem. Soc.* **2002**, *124* (16), 4228-4229. DOI: 10.1021/ja025818u.

(64) Yan, N.; Xiao, C.; Kou, Y. Transition metal nanoparticle catalysis in green solvents. *Coord. Chem. Rev.* **2010**, *254* (9-10), 1179-1218. DOI: 10.1016/j.ccr.2010.02.015.

(65) Silveira, E. T.; Umpierre, A. P.; Rossi, L. M.; Machado, G.; Morais, J.; Soares, G. V.; Baumvol, I. J. R.; Teixeira, S. R.; Fichtner, P. F. P.; Dupont, J. The partial hydrogenation of benzene to cyclohexene by nanoscale ruthenium catalysts in imidazolium ionic liquids. *Chem. - Eur. J.* **2004**, *10* (15), 3734-3740. DOI: 10.1002/chem.200305765.

(66) Chacon, G.; Dupont, J. Arene hydrogenation by metal nanoparticles in ionic liquids. *ChemCatChem* **2019**, *11* (1), 333-341. DOI: 10.1002/cctc.201801363.

(67) Prechtl, M. H. G.; Scariot, M.; Scholten, J. D.; Machado, G.; Teixeira, S. R.; Dupont, J. Nanoscale Ru(0) particles: Arene hydrogenation catalysts in imidazolium ionic liquids. *Inorg. Chem.* **2008**, *47* (19), 8995-9001. DOI: 10.1021/ic801014f.

(68) Abarca, G.; Goncalves, W. D. G.; Albuquerque, B. L.; Dupont, J.; Prechtl, M. H. G.; Scholten, J. D. Bimetallic RuPd nanoparticles in ionic liquids: selective catalysts for the hydrogenation of aromatic compounds. *New J. Chem.* **2021**, *45* (1), 98-103. DOI: 10.1039/d0nj02674c.

(69) Weilhard, A.; Abarca, G.; Viscardi, J.; Prechtl, M. H. G.; Scholten, J. D.; Bernardi, F.; Baptista, D. L.; Dupont, J. Challenging thermodynamics: Hydrogenation of benzene to 1,3-cyclohexadiene by Ru@Pt nanoparticles. *ChemCatChem* **2017**, *9*, 204-211. DOI: 10.1002/cctc.201601196.

(70) Krishnan, D.; Schill, L.; Axet, M. R.; Philippot, K.; Riisager, A. Ruthenium nanoparticles stabilized with methoxy-functionalized ionic liquids: synthesis and structure-performance relations in styrene hydrogenation. *Nanomaterials* **2023**, 13, 1459. https://doi.org/10.3390/nano13091459.

(71) Luska, K. L.; Julis, J.; Stavitski, E.; Zakharov, D. N.; Adams, A.; Leitner, W. Bifunctional nanoparticle-SILP catalysts (NPs@SILP) for the selective deoxygenation of biomass substrates. *Chem. Sci.* **2014**, *5* (12), 4895-4905. DOI: 10.1039/c4sc02033b.

(72) Luska, K. L.; Migowski, P.; El Sayed, S.; Leitner, W. Synergistic interaction within bifunctional ruthenium nanoparticle/SILP catalysts for the selective hydrodeoxygenation of phenols. *Angew. Chem., Int. Ed.* **2015**, *54* (52), 15750-15755. DOI: 10.1002/anie.201508513.

(73) Yan, N.; Yuan, Y.; Dykeman, R.; Kou, Y.; Dyson, P. J. Hydrodeoxygenation of lignin-derived phenols into alkanes by using nanoparticle catalysts combined with bronsted acidic ionic liquids. *Angew. Chem., Int. Ed.* **2010**, *49* (32), 5549-5553. DOI: 10.1002/anie.201001531.

(74) Rengshausen, S.; Etscheidt, F.; Grosskurth, J.; Luska, K. L.; Bordet, A.; Leitner, W. Catalytic hydrogenolysis of substituted diaryl ethers by using ruthenium nanoparticles on an acidic supported ionic liquid phase (Ru@SILP-SO_3H). *Synlett* **2019**, *30* (4), 405-412. DOI: 10.1055/s-0037-1611678.

(75) El Sayed, S.; Bordet, A.; Weidenthaler, C.; Hetaba, W.; Luska, K. L.; Leitner, W. Selective hydrogenation of benzofurans using ruthenium nanoparticles in Lewis acid-modified ruthenium-supported ionic liquid phases. *ACS Catal.* **2020**, *10* (3), 2124-2130. DOI: 10.1021/acscatal.9b05124.

(76) Luska, K. L.; Bordet, A.; Tricard, S.; Sinev, I.; Gruenert, W.; Chaudret, B.; Leitner, W. Enhancing the catalytic properties of ruthenium nanoparticle-SILP catalysts by dilution with iron. *ACS Catal.* **2016**, *6*, 3719-3726. DOI: 10.1021/acscatal.6b00796.

(77) Bordet, A.; El Sayed, S.; Sanger, M.; Boniface, K. J.; Kalsi, D.; Luska, K. L.; Jessop, P. G.; Leitner, W. Selectivity control in hydrogenation through adaptive catalysis using ruthenium nanoparticles on a CO_2-responsive support. *Nat. Chem.* **2021**, *13* (9), 916-922. DOI: 10.1038/s41557-021-00735-w.

(78) Sisodiya-Amrute, S.; Van Stappen, C.; Rengshausen, S.; Han, C.; Sodreau, A.; Weidenthaler, C.; Tricard, S.; DeBeer, S.; Chaudret, B.; Bordet, A.; et al. Bimetallic $M_xRu100\text{-}_x$ nanoparticles (M = Fe, Co)

on supported ionic liquid phases ($M_xRu100-_x$@SILP) as hydrogenation catalysts: Influence of M and M:Ru ratio on activity and selectivity. *J. Catal.* **2022**, *407*, 141-148. DOI: 10.1016/j.jcat.2022.01.030.

(79) Offner-Marko, L.; Bordet, A.; Moos, G.; Tricard, S.; Rengshausen, S.; Chaudret, B.; Luska, K. L.; Leitner, W. Bimetallic nanoparticles in supported ionic liquid phases as multifunctional catalysts for the selective hydrodeoxygenation of aromatic substrates. *Angew. Chem., Int. Ed.* **2018**, *57*, 12721-12726. DOI: 10.1002/anie.201806638.

(80) Goclik, L.; Offner-Marko, L.; Bordet, A.; Leitner, W. Selective hydrodeoxygenation of hydroxyacetophenones to ethyl-substituted phenol derivatives using a FeRu@SILP catalyst. *Chem. Commun.* **2020**, *56* (66), 9509-9512. DOI: 10.1039/d0cc03695a.

(81) Goclik, L.; Walschus, H.; Bordet, A.; Leitner, W. Selective hydrodeoxygenation of acetophenone derivatives using a $Fe_{25}Ru_{75}$@SILP catalyst: a practical approach to the synthesis of alkyl phenols and anilines. *Green Chem.* **2022**, *24* (7), 2937-2945. DOI: 10.1039/d1gc04189d.

(82) Cerezo-Navarrete, C.; David, A. H. G.; Garcia-Zaragoza, A.; Codesal, M. D.; Ona-Burgos, P.; del Rosal, I.; Poteau, R.; Campana, A. G.; Martinez-Prieto, L. M. Ruthenium nanoparticles canopied by heptagon-containing saddle-shaped nanographenes as efficient aromatic hydrogenation catalysts. *Chem. Sci.* **2022**, *13* (44), 13046-13059. DOI: 10.1039/d2sc04228b.

(83) Garcia-Zaragoza, A.; Cerezo-Navarrete, C.; Mollar-Cuni, A.; Ona-Burgos, P.; Mata, J. A.; Corma, A.; Martinez-Prieto, L. M. Tailoring graphene-supported Ru nanoparticles by functionalization with pyrene-tagged N-heterocyclic carbenes. *Catal. Sci. Technol.* **2022**, *12* (4), 1257-1270. DOI: 10.1039/d1cy02063c.

(84) Martinez-Prieto, L. M.; Puche, M.; Cerezo-Navarrete, C.; Chaudret, B. Uniform Ru nanoparticles on N-doped graphene for selective hydrogenation of fatty acids to alcohols. *J. Catal.* **2019**, *377*, 429-437. DOI: 10.1016/j.jcat.2019.07.040.

(85) Cerezo-Navarrete, C.; Mathieu, Y.; Puche, M.; Morales, C.; Concepcion, P.; Martinez-Prieto, L. M.; Corma, A. Controlling the selectivity of bimetallic platinum-ruthenium nanoparticles supported on N-doped graphene by adjusting their metal composition. *Catal. Sci. Technol.* **2021**, *11* (2), 494-505. DOI: 10.1039/d0cy02379e.

(86) Vono, L. L. R.; Broicher, C.; Philippot, K.; Rossi, L. M. Tuning the selectivity of phenol hydrogenation using Pd, Rh and Ru nanoparticles supported on ceria- and titania-modified silicas. *Catal. Today* **2021**, *381*, 126-132. DOI: 10.1016/j.cattod.2020.07.078.

(87) Bertolucci, E.; Bacsa, R.; Benyounes, A.; Raspolli-Galletti, A. M.; Axet, M. R.; Serp, P. Effect of the carbon support on the catalytic activity of Ruthenium-magnetite catalysts for p-chloronitrobenzene hydrogenation. *Chemcatchem* **2015**, *7* (18), 2971-2978. DOI: 10.1002/cctc.201500364.

(88) Axet, M. R.; Conejero, S.; Gerber, I. C. Ligand effects on the selective hydrogenation of nitrobenzene to cyclohexylamine using ruthenium nanoparticles as catalysts. *ACS Appl. Nano Mater.* **2018**, *1*, 5885-5894. DOI: 10.1021/acsanm.8b01549.

(89) Rivera-Carcamo, C.; Leng, F.; Gerber, I. C.; del Rosal, I.; Poteau, R.; Colliere, V.; Lecante, P.; Nechiyil, D.; Bacsa, W.; Corrias, A.; et al. Catalysis to discriminate single atoms from subnanometric ruthenium particles in ultra-high loading catalysts. *Catal. Sci. Technol.* **2020**, *10* (14), 4673-4683. DOI: 10.1039/d0cy00540a.

(90) Moya, A.; Creus, J.; Romero, N.; Aleman, J.; Solans-Monfort, X.; Philippot, K.; Garcia-Anton, J.; Sala, X.; Mas-Balleste, R. Organocatalytic vs. Ru-based electrochemical hydrogenation of nitrobenzene in competition with the hydrogen evolution reaction. *Dalton Trans.* **2020**, *49* (19), 6446-6456. DOI: 10.1039/d0dt01075h.

(91) Yang, H.; Zhang, C.; Gao, P.; Wang, H.; Li, X.; Zhong, L.; Wei, W.; Sun, Y. A review of the catalytic hydrogenation of carbon dioxide into value-added hydrocarbons. *Catal. Sci. Technol.* **2017**, *7* (20), 4580-4598. DOI: 10.1039/c7cy01403a.

(92) Sordakis, K.; Tang, C.; Vogt, L. K.; Junge, H.; Dyson, P. J.; Beller, M.; Laurenczy, G. Homogeneous catalysis for sustainable hydrogen storage in formic acid and alcohols. *Chem. Rev.* **2018**, *118* (2), 372-433. DOI: 10.1021/acs.chemrev.7b00182.

(93) Weilhard, A.; Qadir, M. I.; Sans, V.; Dupont, J. Selective CO_2 hydrogenation to formic acid with multifunctional ionic liquids. *ACS Catal.* **2018**, *8* (3), 1628-1634. DOI: 10.1021/acscatal.7b03931.

(94) Qadir, M. I.; Weilhard, A.; Fernandes, J. A.; de Pedro, I.; Vieira, B. J. C.; Waerenborgh, J. C.; Dupont, J. Selective carbon dioxide hydrogenation driven by ferromagnetic RuFe nanoparticles in ionic liquids. *ACS Catal.* **2018**, *8* (2), 1621-1627. DOI: 10.1021/acscatal.7b03804.

(95) Qadir, M. I.; Bernardi, F.; Scholten, J. D.; Baptista, D. L.; Dupont, J. Synergistic CO_2 hydrogenation over bimetallic Ru/Ni nanoparticles in ionic liquids. *Appl. Catal., B* **2019**, *252*, 10-17. DOI: 10.1016/j.apcatb.2019.04.005.

(96) Louis Anandaraj, S. J.; Kang, L.; DeBeer, S.; Bordet, A.; Leitner, W. Catalytic hydrogenation of CO_2 to formate using ruthenium nanoparticles immobilized on supported ionic liquid phases. *Small* **2023**, 2206806. DOI: 10.1002/smll.202206806.

(97) Mateo, D.; De Masi, D.; Albero, J.; Lacroix, L.-M.; Fazzini, P.-F.; Chaudret, B.; Garcia, H. Synergism of Au and Ru nanoparticles in low-temperature photoassisted CO_2 methanation. *Chem. - Eur. J.* **2018**, *24* (69), 18436-18443. DOI: 10.1002/chem.201803022.

(98) Prakash, G.; Paul, N.; Oliver, G. A.; Werz, D. B.; Maiti, D. C-H deuteration of organic compounds and potential drug candidates. *Chem. Soc. Rev.* **2022**, *51* (8), 3123-3163. DOI: 10.1039/d0cs01496f.

(99) Yang, X.; Ben, H.; Ragauskas, A. J. Recent advances in the synthesis of deuterium-labeled compounds. *Asian J. Org. Chem.* **2021**, *10* (10), 2473-2485. DOI: 10.1002/ajoc.202100381.

(100) Kopf, S.; Bourriquen, F.; Li, W.; Neumann, H.; Junge, K.; Beller, M. Recent developments for the deuterium and tritium labeling of organic molecules. *Chem. Rev.* **2022**, *122* (6), 6634-6718. DOI: 10.1021/acs.chemrev.1c00795.

(101) Sawama, Y.; Monguchi, Y.; Sajiki, H. Efficient H-D exchange reactions using heterogeneous platinum-group metal on carbon-H_2-D_2O system. *Synlett* **2012**, *23* (7), 959-972. DOI: 10.1055/s-0031-1289696.

(102) Pieters, G.; Taglang, C.; Bonnefille, E.; Gutmann, T.; Puente, C.; Berthet, J.-C.; Dugave, C.; Chaudret, B.; Rousseau, B. Regioselective and stereospecific deuteration of bioactive aza compounds by the use of ruthenium nanoparticles. *Angew. Chem., Int. Ed.* **2014**, *53*, 230-234. DOI: 10.1002/anie.201307930.

(103) Valero, M.; Bouzouita, D.; Palazzolo, A.; Atzrodt, J.; Dugave, C.; Tricard, S.; Feuillastre, S.; Pieters, G.; Chaudret, B.; Derdau, V. NHC-stabilized iridium nanoparticles as catalysts in hydrogen isotope exchange reactions of anilines. *Angew. Chem., Int. Ed.* **2020**, *59* (9), 3517-3522. DOI: 10.1002/anie.201914369.

(104) Taglang, C.; Martinez-Prieto, L. M.; del Rosal, I.; Maron, L.; Poteau, R.; Philippot, K.; Chaudret, B.; Perato, S.; Sam Lone, A.; Puente, C.; et al. Enantiospecific C-H activation using ruthenium nanocatalysts. *Angew. Chem., Int. Ed.* **2015**, *54*, 10474-10477. DOI: 10.1002/anie.201504554.

(105) Pfeifer, V.; Certiat, M.; Bouzouita, D.; Palazzolo, A.; Garcia-Argote, S.; Marcon, E.; Buisson, D.-A.; Lesot, P.; Maron, L.; Chaudret, B.; et al. Hydrogen isotope exchange catalyzed by Ru nanocatalysts: labelling of complex molecules containing N-heterocycles and reaction mechanism insights. *Chem. - Eur. J.* **2020**, *26* (22), 4988-4996. DOI: 10.1002/chem.201905651.

(106) Palazzolo, A.; Feuillastre, S.; Pfeifer, V.; Garcia-Argote, S.; Bouzouita, D.; Tricard, S.; Chollet, C.; Marcon, E.; Buisson, D.-A.; Cholet, S.; et al. Efficient access to deuterated and tritiated nucleobase pharmaceuticals and oligonucleotides using hydrogen-isotope exchange. *Angew. Chem., Int. Ed.* **2019**, *58* (15), 4891-4895. DOI: 10.1002/anie.201813946.

(107) Martinez-Prieto, L. M.; Baquero, E. A.; Pieters, G.; Flores, J. C.; de Jesus, E.; Nayral, C.; Delpech, F.; van Leeuwen, P. W. N. M.; Lippens, G.; Chaudret, B. Monitoring of nanoparticle reactivity in solution: interaction of L-lysine and Ru nanoparticles probed by chemical shift perturbation parallels regioselective H/D exchange. *Chem. Commun.* **2017**, *53*, 5850-5853. DOI: 10.1039/c7cc02445b.

(108) Rothermel, N.; Bouzouita, D.; Roether, T.; de Rosal, I.; Tricard, S.; Poteau, R.; Gutmann, T.; Chaudret, B.; Limbach, H.-H.; Buntkowsky, G. Surprising differences of alkane C-H activation catalyzed by ruthenium nanoparticles: Complex surface-substrate recognition? *ChemCatChem* **2018**, *10*, 4243-4247. DOI: 10.1002/cctc.201801022.

(109) Bouzouita, D.; Lippens, G.; Baquero, E. A.; Fazzini, P. F.; Pieters, G.; Coppel, Y.; Lecante, P.; Tricard, S.; Martinez-Prieto, L. M.; Chaudret, B. Tuning the catalytic activity and selectivity of water-soluble bimetallic RuPt nanoparticles by modifying their surface metal distribution. *Nanoscale* **2019**, *11* (35), 16544-16552. DOI: 10.1039/c9nr04149d.

(110) Zuluaga-Villamil, A.; Mencia, G.; Asensio, J. M.; Fazzini, P.-F.; Baquero, E. A.; Chaudret, B. N-Heterocyclic carbene-based iridium and ruthenium/iridium nanoparticles for the hydrogen isotope exchange reaction through C-H bond activations. *Organometallics* **2022**, *41* (22), 3313-3319. DOI: 10.1021/acs.organomet.2c00288.

(111) Gao, L.; Perato, S.; Garcia-Argote, S.; Taglang, C.; Martinez-Prieto, L. M.; Chollet, C.; Buisson, D.-A.; Dauvois, V.; Lesot, P.; Chaudret, B.; et al. Ruthenium-catalyzed hydrogen isotope exchange of C(sp^3)-H bonds directed by a sulfur atom. *Chem. Commun.* **2018**, *54*, 2986-2989. DOI: 10.1039/c8cc00653a.

(112) Palazzolo, A.; Naret, T.; Daniel-Bertrand, M.; Buisson, D.-A.; Tricard, S.; Lesot, P.; Coppel, Y.; Chaudret, B.; Feuillastre, S.; Pieters, G. Tuning the reactivity of a heterogeneous catalyst using N-heterocyclic carbene ligands for C-H activation reactions. *Angew. Chem., Int. Ed.* **2020**, *59* (47), 20879-20884. DOI: 10.1002/anie.202009258.

(113) Creus, J.; De Tovar, J.; Romero, N.; Garcia-Anton, J.; Philippot, K.; Bofill, R.; Sala, X. Ruthenium nanoparticles for catalytic water splitting. *ChemSusChem* **2019**, *12* (12), 2493-2514. DOI: 10.1002/cssc.201900393.

(114) Romero, N.; Creus, J.; Garcia-Anton, J.; Bofill, R.; Sala, X. Rebirth of ruthenium-based nanomaterials for the hydrogen evolution reaction. In *Nanoparticles in catalysis*, Roucoux, A., Philippot, K. Eds.; 2021; pp 257-277.

(115) Creus, J.; Drouet, S.; Surinach, S.; Lecante, P.; Colliere, V.; Poteau, R.; Philippot, K.; Garcia-Anton, J.; Sala, X. Ligand-capped Ru nanoparticles as efficient electrocatalyst for the hydrogen evolution reaction. *ACS Catal.* **2018**, *8* (12), 11094-11102. DOI: 10.1021/acscatal.8b03053.

(116) Creus, J.; Mallon, L.; Romero, N.; Bofill, R.; Moya, A.; Fierro, J. L. G.; Mas-Balleste, R.; Sala, X.; Philippot, K.; Garcia-Anton, J. Ruthenium nanoparticles supported on carbon microfibers for hydrogen evolution electrocatalysis. *Eur. J. Inorg. Chem.* **2019**, *2019* (15), 2071-2077. DOI: 10.1002/ejic.201801438.

(117) Mallon, L.; Cerezo-Navarrete, C.; Romero, N.; Puche, M.; Garcia-Anton, J.; Bofill, R.; Philippot, K.; Martinez-Prieto, L. M.; Sala, X. Ru nanoparticles supported on alginate-derived graphene as hybrid electrodes for the hydrogen evolution reaction. *New J. Chem.* **2022**, *46* (1), 49-56. DOI: 10.1039/d1nj05215b.

(118) Romero, N.; Guerra, R. B.; Gil, L.; Drouet, S.; Salmeron-Sanchez, I.; Illa, O.; Philippot, K.; Natali, M.; Garcia-Anton, J.; Sala, X. TiO_2-mediated visible-light-driven hydrogen evolution by ligand-capped Ru nanoparticles. *Sustainable Energy Fuels* **2020**, *4* (8), 4170-4178. DOI: 10.1039/d0se00446d.

(119) Yamada, Y.; Miyahigashi, T.; Kotani, H.; Ohkubo, K.; Fukuzumi, S.-I. Photocatalytic hydrogen evolution under highly basic conditions by using Ru nanoparticles and 2-Phenyl-4-(1-naphthyl)quinolinium ion. *J. Am. Chem. Soc.* **2011**, *133* (40), 16136-16145. DOI: 10.1021/ja206079e.

(120) Alvarez-Prada, I.; Nguyen, A. D.; Romero, N.; Hou, H.; Benazzi, E.; Escriche, L.; Acharjya, A.; Thomas, A.; Schwarze, M.; Schomacker, R.; et al. Insights into the light-driven hydrogen evolution reaction of mesoporous graphitic carbon nitride decorated with Pt or Ru nanoparticles. *Dalton Trans.* **2022**, *51* (2), 731-740. DOI: 10.1039/d1dt03006j.

(121) Alvarez-Prada, I.; Peral, D.; Song, M.; Munoz, J.; Romero, N.; Escriche, L.; Acharjya, A.; Thomas, A.; Schomacker, R.; Schwarze, M.; et al. Ruthenium nanoparticles supported on carbon-based nanoallotropes as co-catalyst to enhance the photocatalytic hydrogen evolution activity of carbon nitride. *Renewable Energy* **2021**, *168*, 668-675. DOI: 10.1016/j.renene.2020.12.070.

(122) Martí, G., Mallón, L., Romero, N., Francàs, L., Bofill, R., Philippot; K., G.-A., J. and Sala, X; Martí , G.; Mallón , L.; Romero , N.; Francàs , L.; Bofill , R.; Philippot , K.; García-Antón , J.; Sala, X. Surface-functionalized nanoparticles as catalysts for artificial photosynthesis. *Adv. Energy Mater.* **2023**, 2300282. DOI: 10.1002/aenm.202300282.

(123) Qadir, M. I.; Baptista, D. L.; Dupont, J. Effect of support nature on ruthenium-catalyzed allylic oxidation of cycloalkenes. *Catal. Lett.* **2022**, *152* (10), 3058-3065. DOI: 10.1007/s10562-021-03880-6.

(124) Molinillo, P.; Lacroix, B.; Vattier, F.; Rendon, N.; Suarez, A.; Lara, P. Reduction of N_2O with hydrosilanes catalysed by RuSNS nanoparticles. *Chem. Commun.* **2022**, *58* (51), 7176-7179. DOI: 10.1039/d2cc01470j.

(125) Kalsi, D.; Louis Anandaraj, S. J.; Durai, M.; Weidenthaler, C.; Emondts, M.; Nolan, S. P.; Bordet, A.; Leitner, W. One-pot multicomponent synthesis of allyl and alkylamines using a catalytic system composed of ruthenium nanoparticles on copper N-heterocyclic carbene-modified silica. ACS Catal. 2022, 12 (24), 14902-14910. DOI: 10.1021/acscatal.2c04044

(126) Qadir, M. I.; Castegnaro, M. V.; Selau, F. F.; Samperi, M.; Fernandes, J. A.; Morais, J.; Dupont, J. Catalytic semi-water-gas shift reaction: A simple green path to formic acid fuel. *ChemSusChem* **2020**, *13* (7), 1817-1824. DOI: 10.1002/cssc.201903417.